RAPID MACROCELL TESTS OF ASTM A775, A615, and A1035 REINFORCING BARS

By
W. Joseph Sturgeon
Matthew O'Reilly
David Darwin
JoAnn Browning

A Report on Research Sponsored by the

EPOXY INTEREST GROUP
OF THE CONCRETE REINFORCING STEEL INSTITUTE

Structural Engineering and Engineering Materials
SL Report 10-4
November 2010

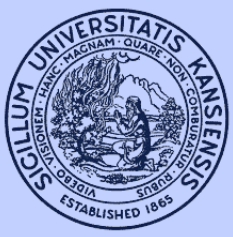

THE UNIVERSITY OF KANSAS CENTER FOR RESEARCH, INC.
2385 Irving Hill Road, Lawrence, Kansas 66045-7563

RAPID MACROCELL TESTS OF ASTM A775, A615, and A1035 REINFORCING BARS

By

W. Joseph Sturgeon

Matthew O'Reilly

David Darwin

JoAnn Browning

Research supported by the

EPOXY INTEREST GROUP
OF THE CONCRETE REINFORCING STEEL INSTITUTE

Structural Engineering and Engineering Materials
SL Report 10-4

THE UNIVERSITY OF KANSAS CENTER FOR RESEARCH, INC.
LAWRENCE, KANSAS
November 2010

ABSTRACT

The corrosion performance of epoxy-coated steel meeting the requirements of ASTM A775 with the coating in an undamaged condition and two damaged conditions (0.04% and 0.83% damaged area) is evaluated in accordance with Annexes A1 and A2 of ASTM 955 and compared with the corrosion performance of conventional reinforcing steel meeting the requirements of ASTM A615 steel and low-carbon, chromium steel meeting the requirements of A1035, with the latter in both the as-received and pickled conditions.

Epoxy-coated bars provide significantly better corrosion performance than conventional reinforcing steel. The macrocell corrosion rates for bars with a damaged area equal to 0.04% of the area exposed to the solutions in the test are relatively low, and are, on average, similar to those observed for the undamaged epoxy-coated bars. Both undamaged and 0.04% damaged area epoxy-coated specimens meet the requirements for stainless steels specified in Annexes A1 and A2 of ASTM 955, with an average corrosion rate not exceeding 0.25 μm/yr and the corrosion rate of no individual specimen exceeding 0.50 μm/yr. The macrocell corrosion rates for bars with a damaged area equal to 0.83% of the area exposed to the solutions in the test average 1 to 1.5 μm/yr based on total bar area under the severe exposure conditions provided. Conventional and A1035 steel exhibit average values near 30 μm/yr for and 20 μm/yr, respectively. Pickling provides initial protection to A1035 steel bars, and to some bars for the duration of the test, but once corrosion initiates, corrosion appears to be similar to that observed on non-pickled bars.

Keywords: chlorides, concrete, corrosion, epoxy coating, macrocell, reinforcing steel

ACKNOWLEDGEMENTS

The research described in this report was supported by the Epoxy Interest Group of the Concrete Reinforcing Steel Institute.

INTRODUCTION

This report describes rapid macrocell tests performed in accordance with Annexes A1 and A2 of ASTM A955-10 that are used to evaluate the corrosion performance of epoxy-coated steel meeting the requirements of ASTM A775 in the undamaged condition and two damaged conditions (0.04% and 0.83% damaged area) and compare that performance with that of conventional reinforcing steel meeting the requirements of ASTM A615 and low-carbon, chromium steel meeting the requirements of A1035, with the latter in both the as-received and pickled conditions. Six specimens of each type are tested.

EXPERIMENTAL WORK

Materials

Tests were performed on epoxy-coated reinforcement (ECR) in the undamaged condition and with damage to 0.04% and 0.83% of the exposed area, as well as on conventional steel reinforcement meeting the requirements of ASTM A615 used to make the epoxy-coated bars and bars meeting the requirements of A1035 in the as-received and pickled conditions. All tests were performed on No. 5 (No. 16) reinforcing bars.

The ECR bars were coated with a fusion-bonded epoxy meeting the requirements of ASTM A775.

The bars were inspected upon receipt, and the conventional steel and ECR were found to be in good condition. The A1035 exhibited significant corrosion, as shown in Figure 1. As a result, macrocell tests were performed on the A1035 bars after pickling, as well as in the as-received condition.

Pickling of the A1035 steel was performed at the University of Kansas. The pickling procedure consisted of submerging the specimens in a solution of 2.5% nitric acid and 0.5% hydrofluoric acid for five minutes at room temperature (72º F, 22º C) followed by rinsing with deionized water. After initial pickling, grooves running along the length of the specimens were observed, as shown in Figure 2. The specimens were then grit-blasted with silica-carbide and re-pickled in the same manner as before, but the grooves remained.

To protect the exposed steel at the submerged ends of the ECR specimens, one end of each test bar was coated with two-part epoxy patch material, which was left to dry overnight. Next, the bars were given a fresh coat of the two-part epoxy patch material on the same end and then fitted with a 0.5-in. (12.5-mm) deep vinyl cap that was coated with the two-part epoxy patch material on the inside. For tests using damaged ECR, the coating on each bar was penetrated using four holes drilled to a depth of 16 mils (0.4 mm) from the epoxy surface – two per side with one located 1 in. (25.4 mm) from the bottom end of the

Figure 1: A1035 steel in the as-received condition exhibit corrosion on the surface of the bars.

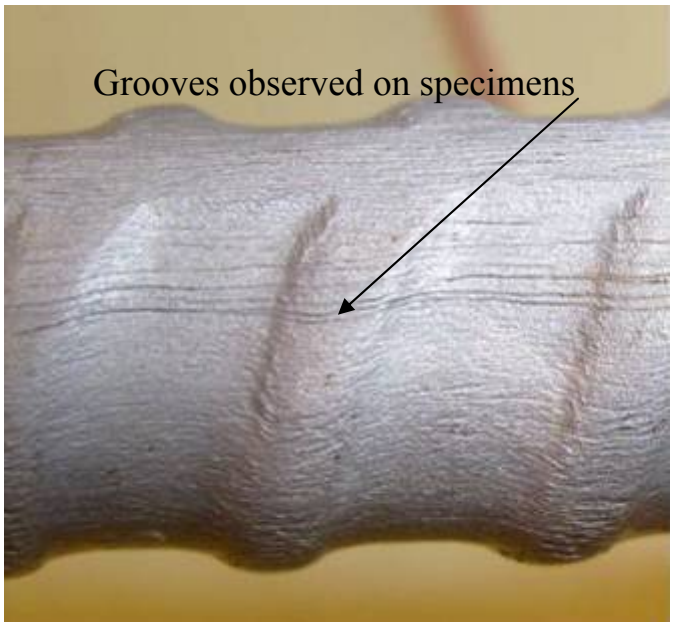

Figure 2: Close-up of length-wise grooves in A1035 steel specimen.

bar and the second spaced 1 in. (25.4 mm) from the first. 1/8-in. (3.2-mm) and 0.7-mm (0.028-in.) diameter drill bits were used to achieve 0.83% and 0.04% damage, respectively.

The chemical composition of the steel used for the conventional steel and the ECR bars is given in Table 1. The chemical composition of the A1035 bars was not available.

Table 1: Chemical composition of conventional steel (provided by manufacturer).

Material Composition, percent												
Cr	**Ni**	**C**	**Mn**	**P**	**S**	**Mo**	**Si**	**Cu**	**Cb**	**V**	**Al**	**Sn**
0.220	0.210	0.390	0.970	0.016	0.034	0.085	0.240	0.310	0.002	0.002	0.002	0.018

Experimental Procedures

Rapid Macrocell Test

Six specimens were tested for each of the six series included in this study in accordance with the rapid macrocell test outlined in Annexes A1 and A2 of ASTM A955/A955M-10 and detailed in Figures 3 and 4. The original test configuration is shown in Figure 3, while the

modified configuration is shown in Figure 4. In the original configuration, the specimens are supported at holes through the container lid, which is cut to fit inside the container. Based upon previous testing observations, the contact point where the specimens occasionally rest against the lid creates a crevice that accelerates local corrosion. To remedy this, the test has been modified. In the new configuration, the specimens are supported by the attached wire. The wire is held in place by slots cut in the container lid, which is placed on top of the container. The bars in the conventional, A1035 as-received, and all ECR series were tested using the original configuration shown in Figure 3. The pickled A1035 steel series used the modified configuration shown in Figure 4.

Each bar used in the rapid macrocell test is 5 in. long and is drilled and tapped at one end to accept a 0.5-in., 10-24 stainless steel machine screw. Conventional and A1035 bars, both as-received and pickled, are cleaned prior to testing with acetone to remove oil and surface contaminants introduced by machining. All ECR specimens are cleaned prior to testing in a similar manner, except that soap and water is used in place of acetone. A length of 16-gauge

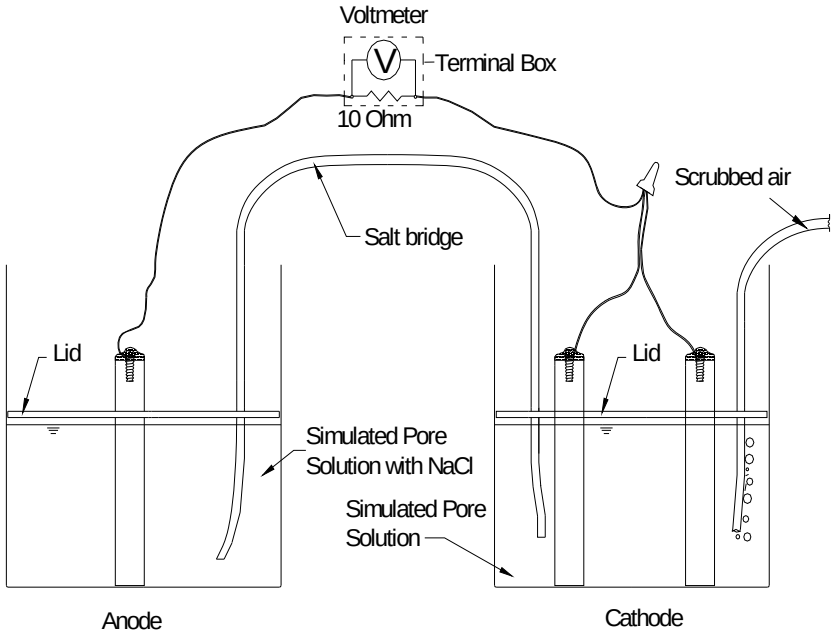

Figure 3: Original test setup where specimens are supported by the container lids.

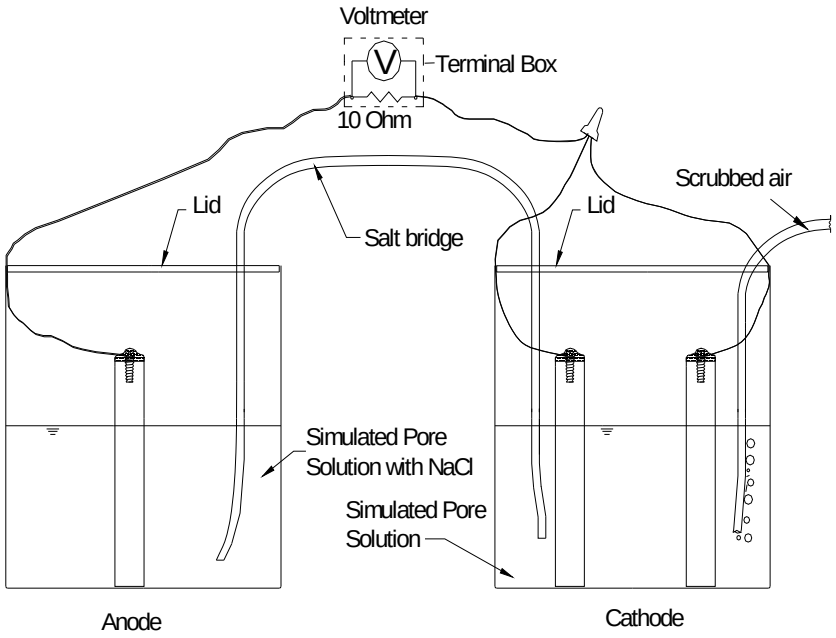

Figure 4: Modified test setup where specimens are supported by the container lids.

insulated copper wire is attached to each bar via the machine screw. The electrical connection is coated with the two-part epoxy patch material to protect the wire from corrosion.

Extra precautions were taken when preparing the ECR specimens. A woven fabric and rubber protective sheath are used when clamping the bars in the lathe to drill and tap the bars. To grip an ECR bar in the lathe, the clamp must penetrate the rubber layer, while the inner fabric protects the epoxy. On occasion, however, the clamp will penetrate the epoxy coating or locally compress the coating but not penetrate to the steel. Any perforations in the coating that expose steel are sealed prior to testing using the same epoxy patch material that is used to coat the electrical connections. When selecting anode and cathode bars, bars with patches are used as cathodes to minimize irregularities on the anode bars.

A single rapid macrocell specimen consists of an anode and a cathode. The liquid level in this series of tests is adjusted to provide a consistent area of specimen exposed to solution. The

ECR specimens are submerged to a depth of 3.5 in. (89 mm) so that, with the 0.5 in. (12.5 mm) vinyl cap on the end, the specimen has an exposure equal to that of an uncapped bar at 3 in. Likewise, the conventional and A1035 specimens are submerged to a depth of 2.84 in. to account for exposure of the bottom of the bars with no vinyl caps.

The cathode consists of two bars submerged in simulated pore solution in a plastic container, as shown in Figures 3 and 4. One liter of pore solution consists of 974.8 g of distilled water, 18.81 g of potassium hydroxide (KOH), and 17.87 g of sodium hydroxide (NaOH). The solution has a pH of about 13.4. Air, scrubbed to remove carbon dioxide, is bubbled into the cathode solution. The anode consists of a single bar submerged in a solution consisting of simulated pore solution and 15 percent sodium chloride (NaCl). The "salt" solution is prepared by adding 172.1 g of NaCl to one liter of pore solution. The solutions are changed every five weeks to limit the effects of carbonation. The anode and cathode are connected electrically across a 10-ohm resistor. A potassium chloride (KCl) salt bridge provides an ionic connection between the anode and the cathode (Figures 3 and 4).

The corrosion rate is calculated based on the voltage drop across the 10-ohm resistor using Faraday's equation:

$$\text{Rate} = K\frac{V \cdot m}{n \cdot F \cdot D \cdot R \cdot A} \qquad (1)$$

where the Rate is given in μm/yr, and

K = conversion factor = $31.5 \cdot 10^4$ amp·μm ·sec/μA·cm·yr

V = measured voltage drop across resistor, millivolts

m = atomic weight of the metal (for iron, m = 55.8 g/g-atom)

n = number of ion equivalents exchanged (for iron, n = 2 equivalents)

F = Faraday's constant = 96485 coulombs/equivalent

D = density of the metal, g/cm^3 (for iron, D = 7.87 g/cm^3)

R = resistance of resistor, ohms = 10 ohms for the test

A = surface area of anode exposed to solution, 38.0 cm^2

Using the values listed above, the corrosion rate simplifies to:

$$\text{Rate} = 30.52\ V \qquad (2)$$

Because of inherent electrical noise, voltage readings between positive and negative 0.003 mV are rounded to zero. Thus, apparent corrosion rates between positive and negative 0.092 μm/yr are set to zero.

ASTM A955 addresses the requirements for stainless steel reinforcing bars. To qualify under the provisions of Annexes A1 and A2, no individual reading may exceed 0.50 μm/yr, and the average corrosion rate of all specimens may not exceed 0.25 μm/yr. In both cases, the corrosion current must be such as to indicate net corrosion at the anode. Current indicating a "negative" value of corrosion, independent of value, does not indicate corrosion of the anode and is caused by minor differences in oxidation rate between the single anode bar and the two cathode bars.

In addition to measuring the voltage drop across the 10-ohm resistor, which is used to calculate the corrosion rate, the corrosion potentials at the anode and cathode are measured using a saturated calomel electrode (SCE). Readings are taken daily for the first week and weekly thereafter.

RESULTS

Conventional and A1035 Steel

The individual corrosion rates of the six conventional steel specimens are shown in Figure 5, and the average corrosion rate is shown in Figure 6. The rates range from 10 to nearly

80 µm/yr, with an average of about 30 µm/yr, which is typical of conventional steel reinforcement in the rapid macrocell test. The error bars shown in Figure 6 represent one standard deviation above and below the mean value based on the corrosion rates for the individual specimens.

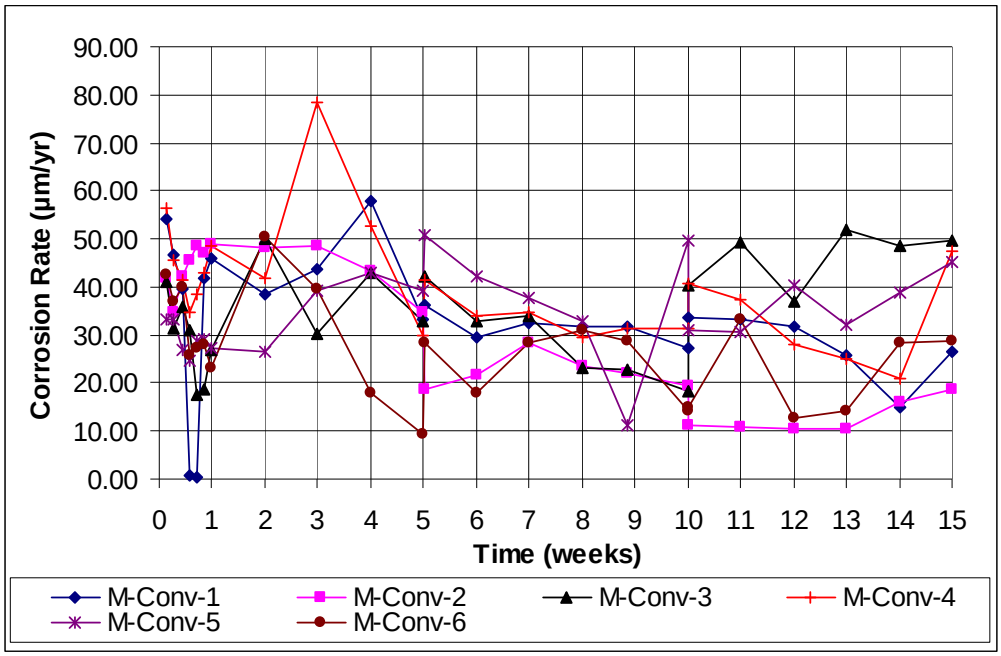

Figure 5: Individual corrosion rate of conventional steel, Specimens 1-6.

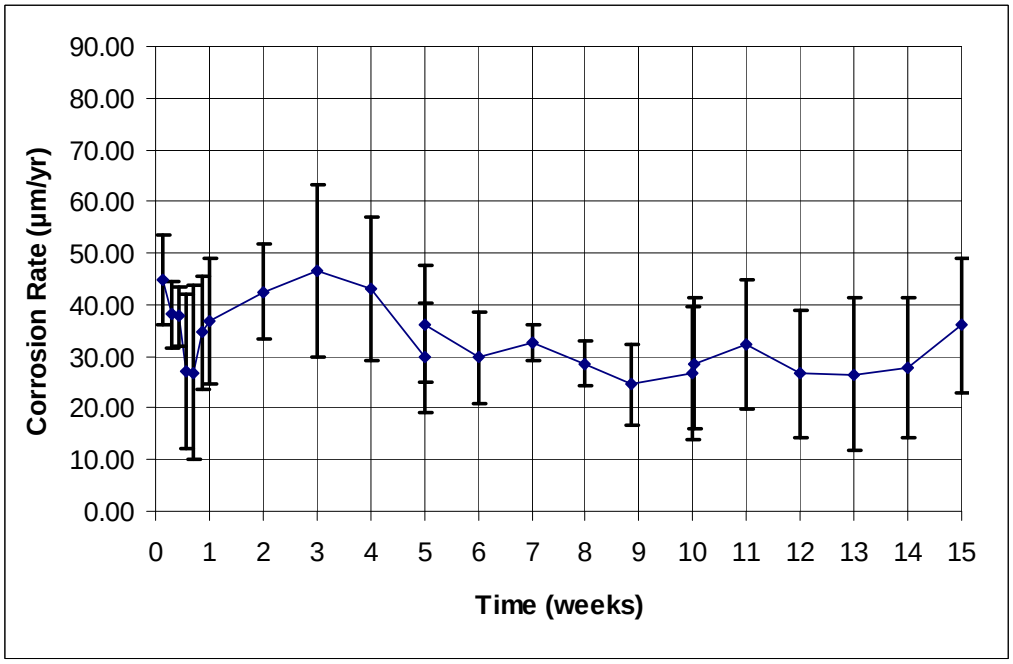

Figure 6: Average corrosion rate of conventional steel, Specimens 1-6.

The corrosion rates for the individual as-received A1035 steel specimens varied between 10 and 40 μm/yr, as shown in Figure 7. The average corrosion rate for the specimens, shown in Figure 8, is 20 μm/yr, which is equal to about two-thirds of the value for conventional steel. The pickled A1035 steel individual and average corrosion rates are shown in Figures 9 and 10, respectively. Initially, the pickling process passivates the steel, providing protection and reducing corrosion rates to a range of 0 to 5 μm/yr. But, as the tests progress, one specimen exhibits more severe corrosion at week five, and two others initiate at week 10. Once corrosion initiates, the pickled-bars tend to corrode at a rate similar to that of the as-received A1035 bars.

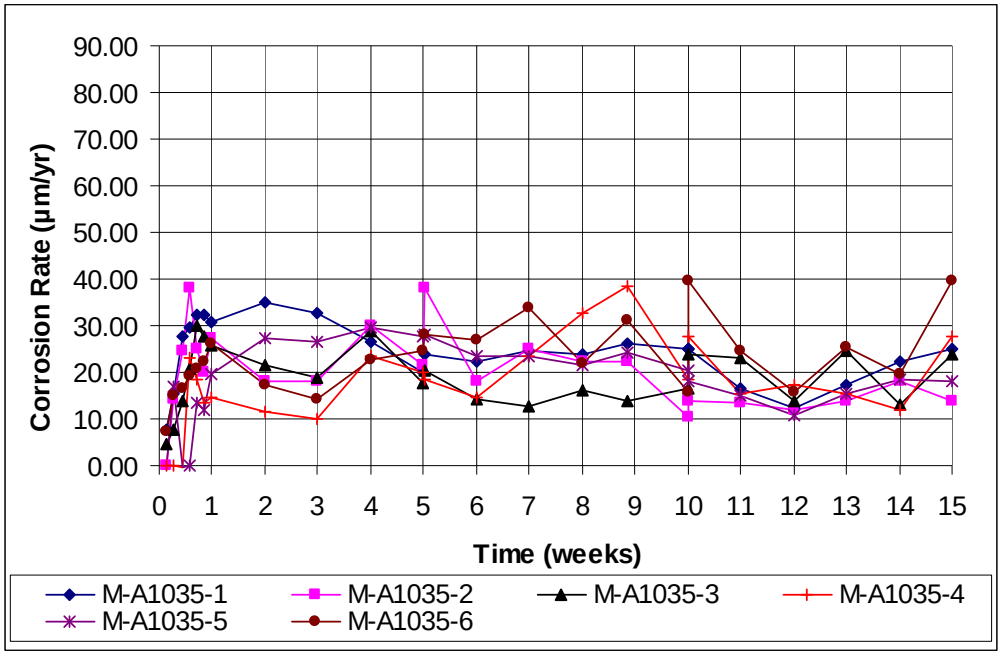

Figure 7: Individual corrosion rate of as-received A1035 steel, Specimens 1-6.

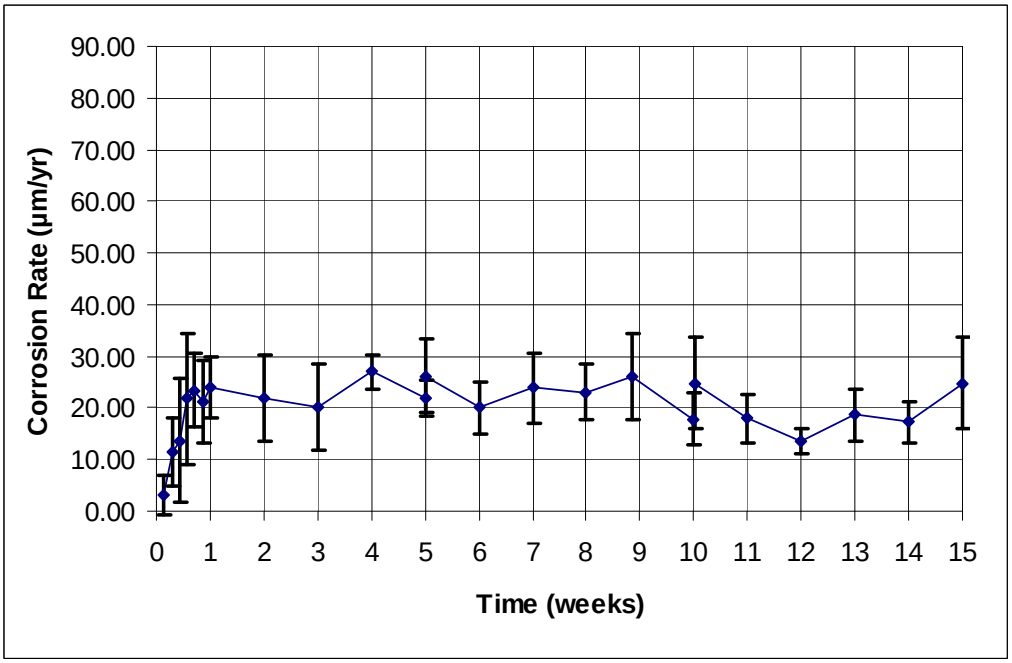

Figure 8: Average corrosion rate of as-received A1035 steel, Specimens 1-6.

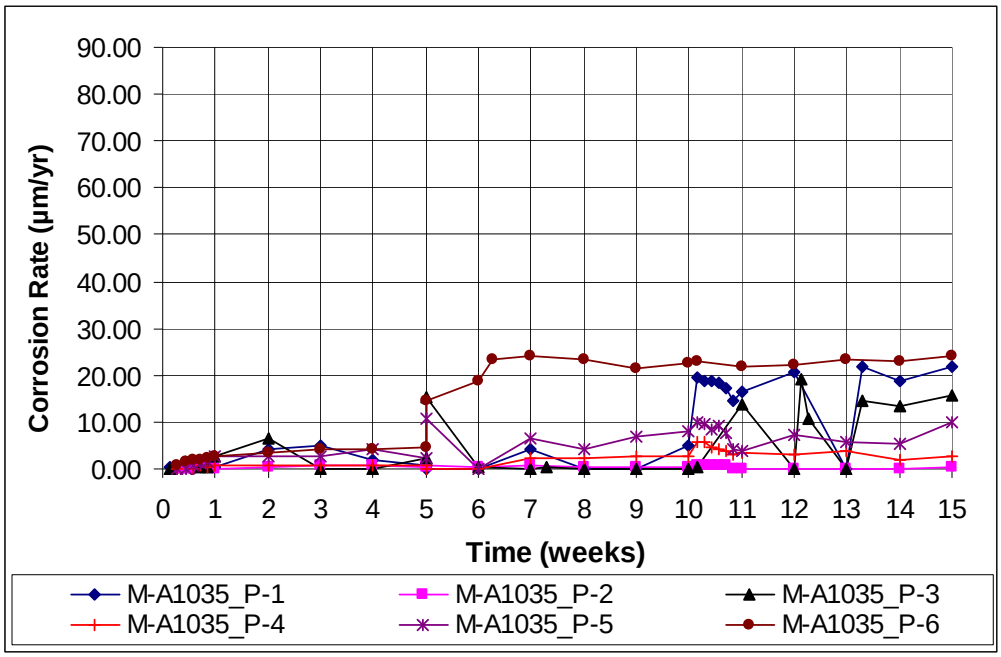

Figure 9: Individual corrosion rate of pickled A1035 steel, Specimens 1-6.

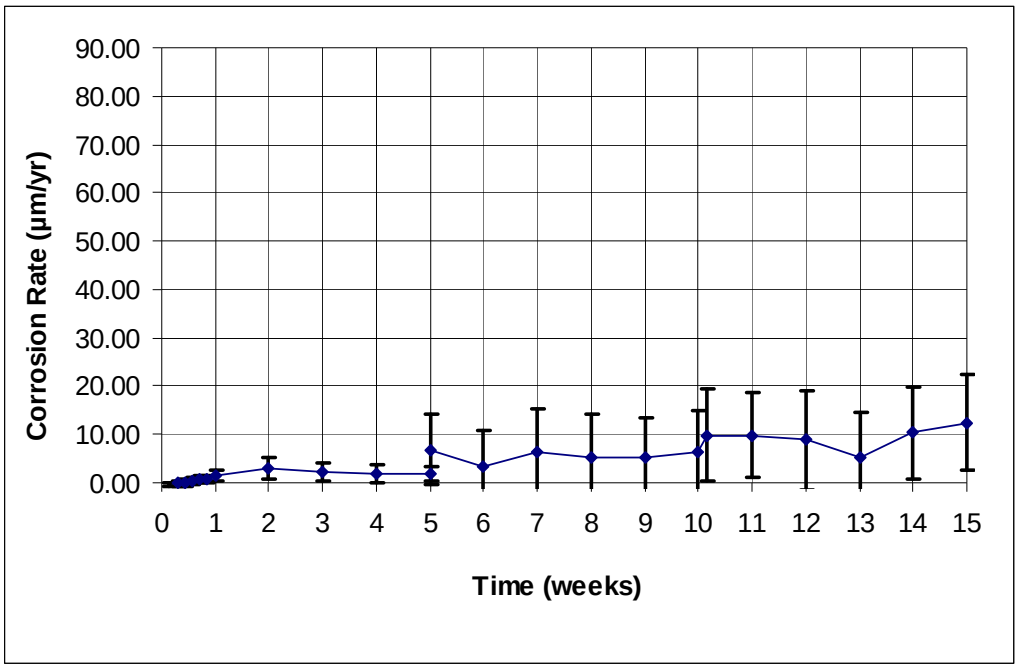

Figure 10: Average corrosion rate of pickled A1035 steel, Specimens 1-6.

Individual corrosion potential data taken with respect to a saturated calomel electrode (SCE) for the bars in salt solution (anode) and bars in pore solution (cathode) are shown in Figures 11 and 12, respectively, for conventional steel. The bars in salt solution show tightly bunched potentials around −0.500 V verses the SCE. In contrast, the bars in pore solution have slightly more scattered potentials, shown in Figure 12, generally within the range of −0.200 to −0.250 V. Overall, the average potential, shown in Figure 13, is more negative for the bars in salt solution than for bars in the pore solution by 0.250 to 0.300 V for most of the test.

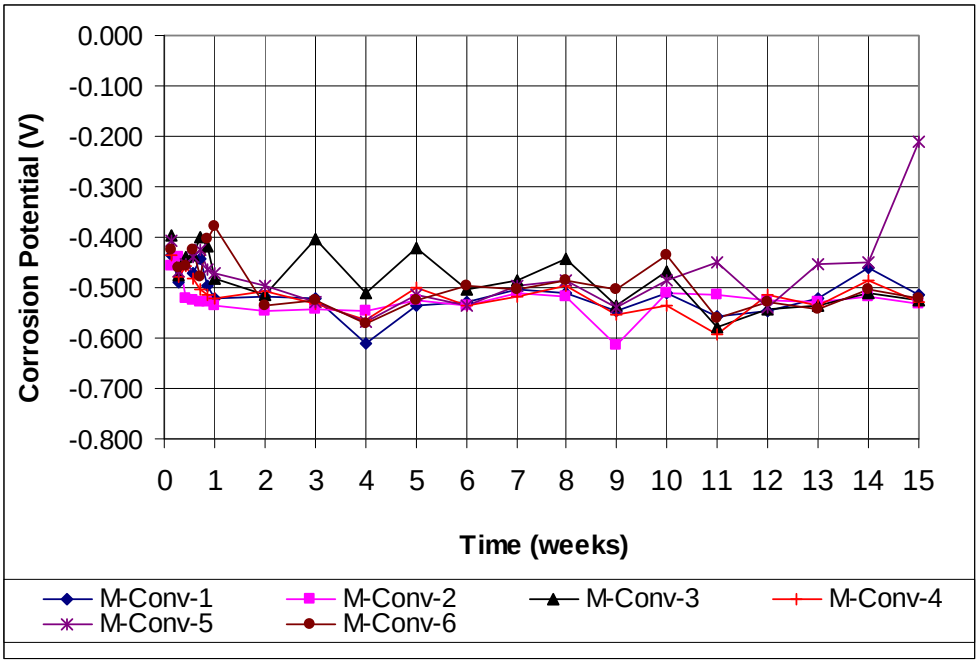

Figure 11: Individual corrosion potentials with respect to SCE. Conventional steel bars in salt solution (anode), specimens 1-6.

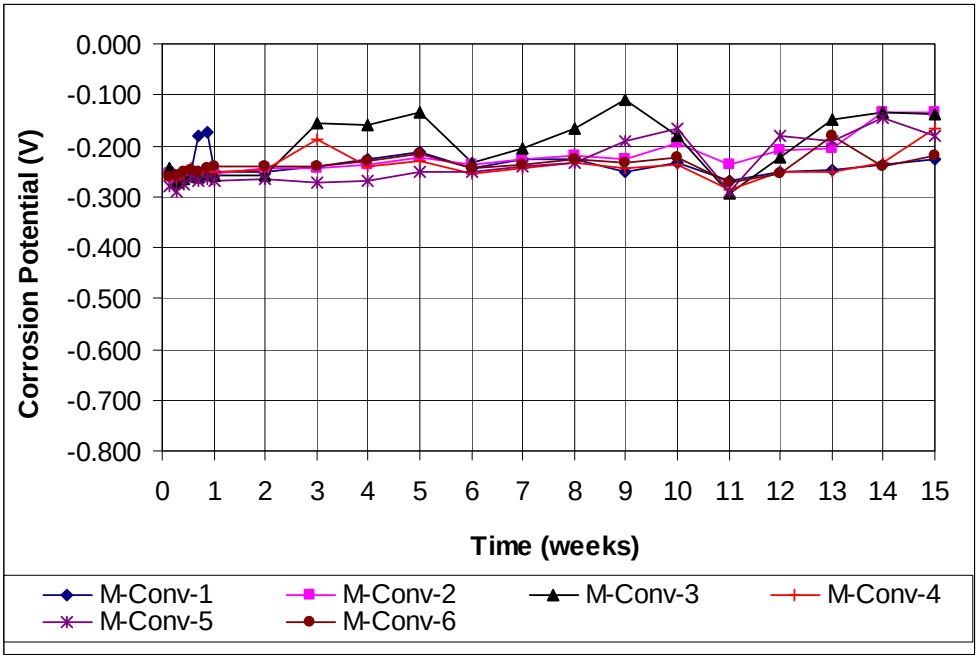

Figure 12: Individual corrosion potentials with respect to SCE. Conventional steel bars in pore solution (cathode), specimens 1-6.

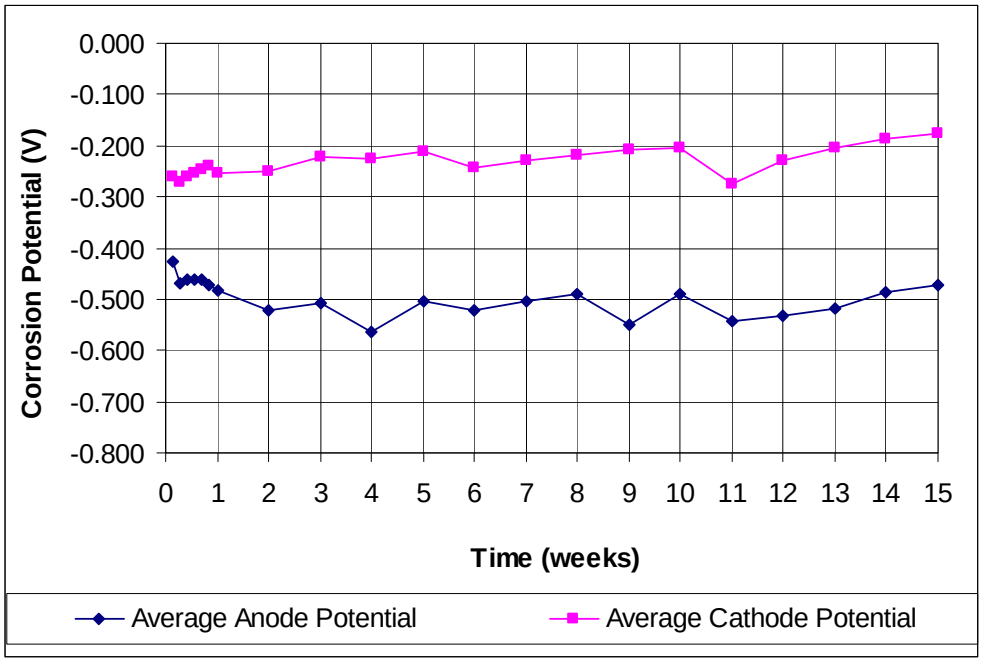

Figure 13: Average corrosion potentials with respect to SCE. Conventional steel bars, specimens 1-6.

The individual corrosion potentials with respect to an SCE for the as-received A1035 steel are shown in Figures 14 and 15 for the anode and cathode bars, respectively. Both the anode and the cathode potentials are tightly bunched and are comparable to those shown for the conventional steel. The anode potentials are close to −0.500 V for most of the test, and the cathode potentials are between −0.200 to −0.250 V. The average potentials, shown in Figure 16, exhibit an anode potential more negative than the cathode potential by -0.250 to -0.300 V throughout the test.

ASTM C876 states that a potential more negative than −0.275 V with respect to an SCE (−0.350 with respect to a copper/copper sulfate electrode) indicates a 90% probability that corrosion is occurring. Two important differences between this macrocell test (all A1035 specimens) and ASTM C876 prevent a direct comparison of this test to ASTM C876: the

reinforcement used is not a conventional steel alloy, and the bars were placed in a pore solution, not concrete.

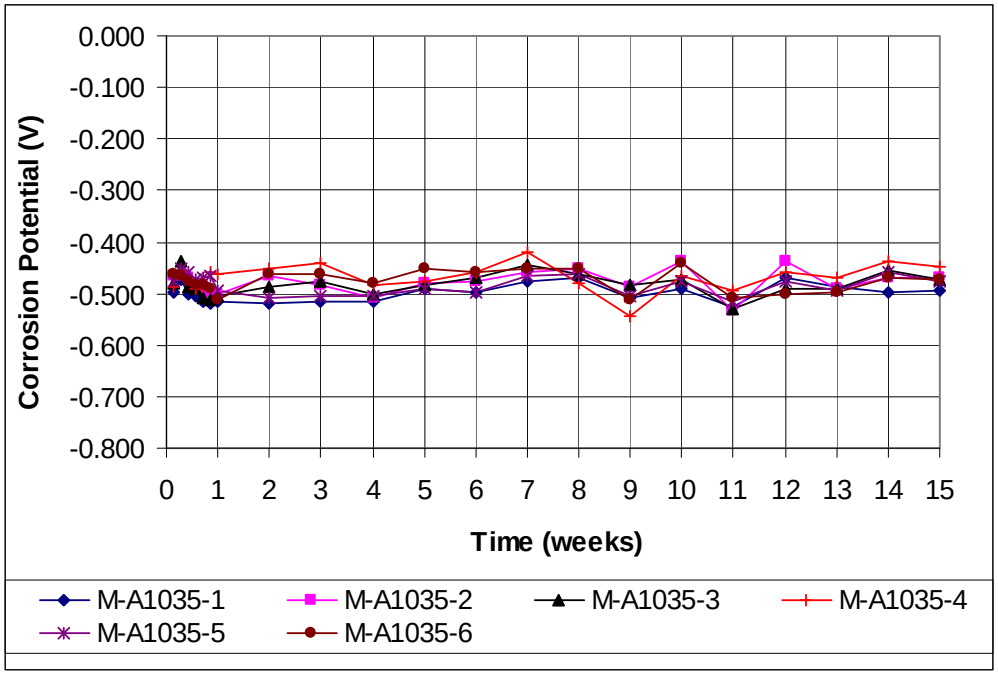

Figure 14: Individual corrosion potentials with respect to SCE. As-received A1035 steel bars in salt solution (anode), specimens 1-6.

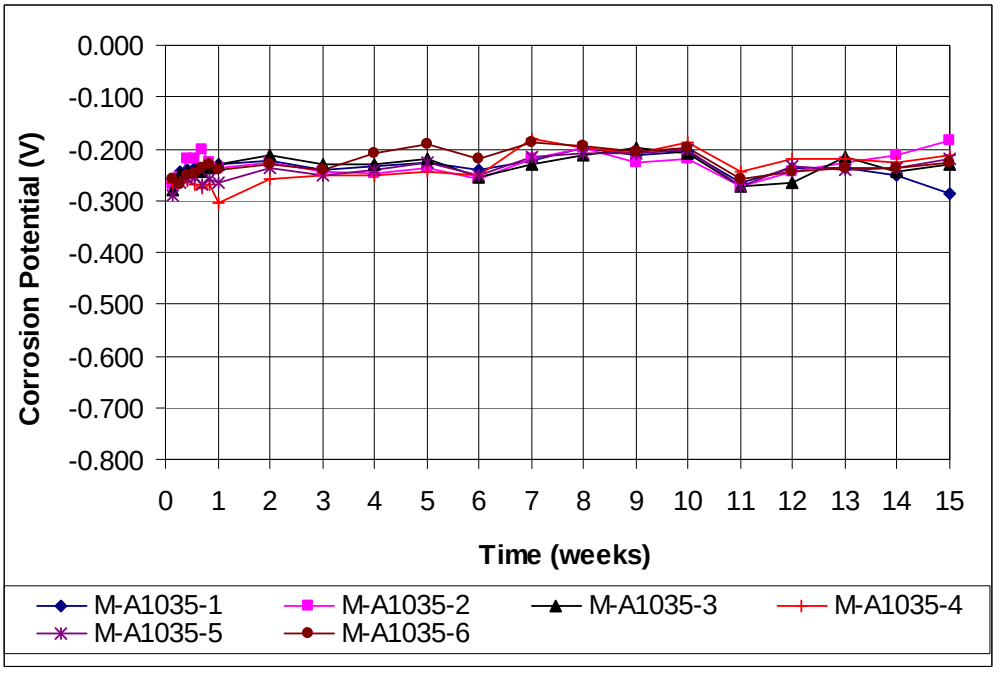

Figure 15: Individual corrosion potentials with respect to SCE. As-received A1035 steel bars in pore solution (cathode), specimens 1-6.

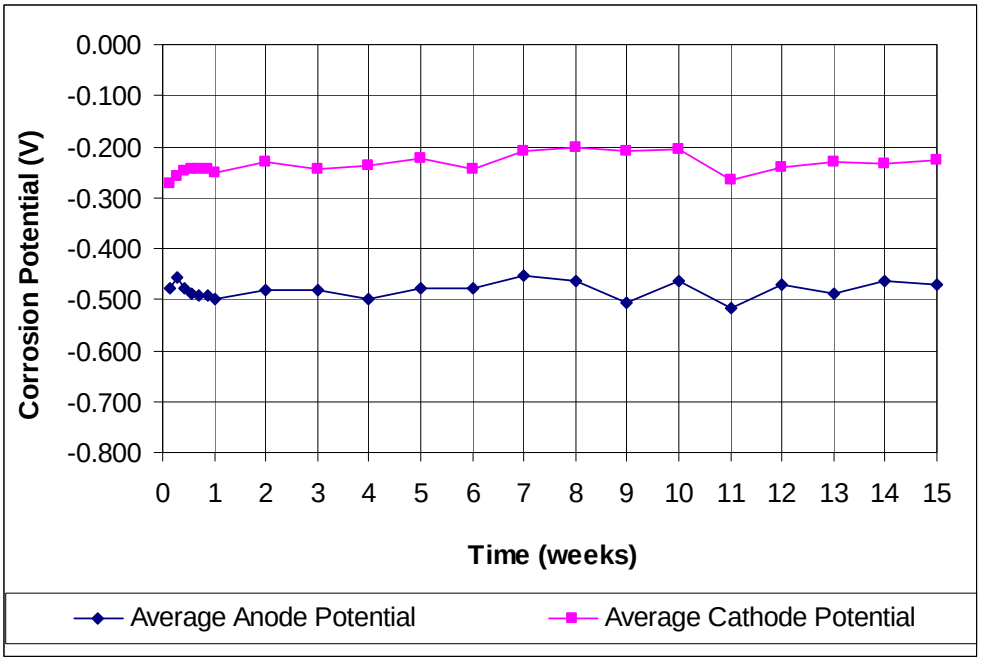

Figure 16: Average corrosion potentials with respect to SCE. As-received A1035 steel bars, specimens 1-6.

For the pickled A1035 steel, the corrosion potentials, shown in Figures 17 and 18, are more scattered than for either the as-received A1035 or the conventional steel specimens. The anode potentials vary from −0.200 to −0.500 V during the test. The cathode potentials show more limited variation and range from −0.100 to −0.250 V. The average potentials are shown in Figure 19. It can be observed that pickling results in initial passivation but the effect is lost as the test progresses. There is also a correlation between the anode potentials of specimens, as shown in Figure 17, and the corrosion rates, as shown in Figure 9; specimens 2 and 4 exhibit corrosion potentials more positive than −0.370 V and corrosion rates below 6 μm/yr throughout the test, while specimens 1, 3, 5, and 6 exhibit corrosion potentials more negative than −0.450 V and corrosion rates between 10 and 24 μm/yr by the end of the test. Specimen 2 consistently had the most positive corrosion potential and the lowest corrosion rate. By the end of the test, the anode corrosion potentials for these specimens have reached –0.500 V for four of the six specimens.

Likewise, the corrosion rates for these specimens are elevated, resulting in similar corrosion rates to those observed for the as-received A1035 specimens.

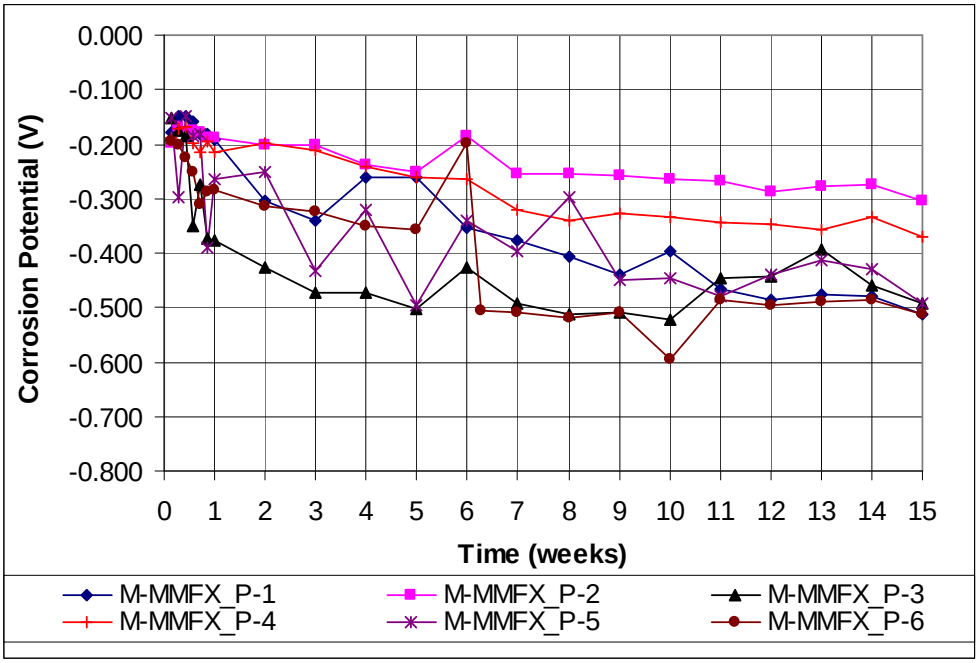

Figure 17: Individual corrosion potential with respect to SCE. Pickled A1035 steel bars in salt solution (anode), specimens 1-6.

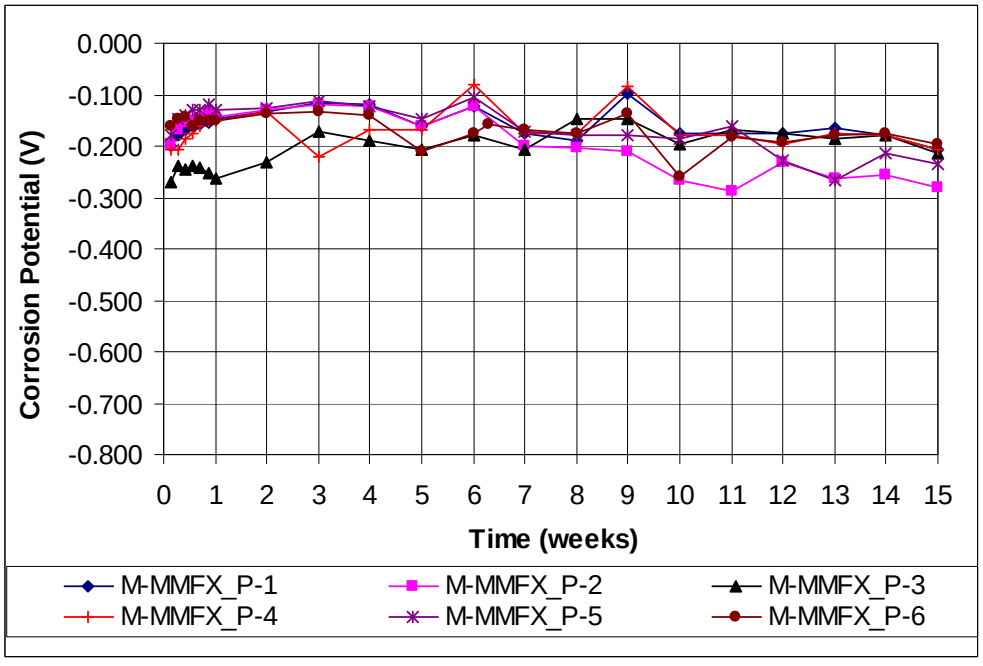

Figure 18: Individual corrosion potential with respect to SCE. Pickled A1035 steel bars in pore solution (cathode), specimens 1-6.

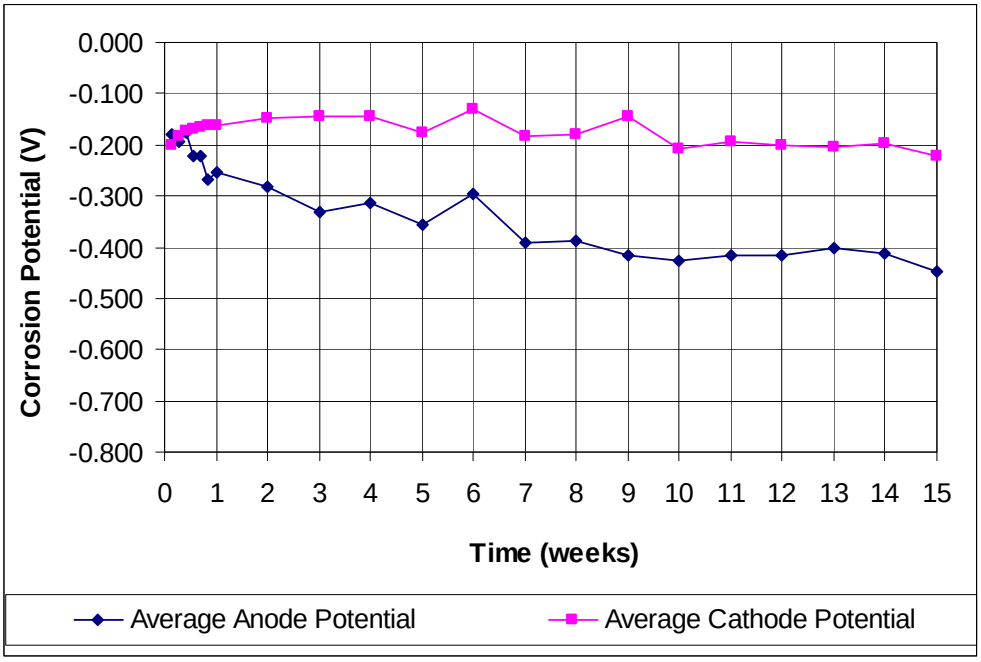

Figure 19: Average corrosion potential with respect to SCE. Pickled A1035 steel bars, specimens 1-6.

All conventional, as-received A1035, and pickled A1035 steel specimens exhibit corrosion during the test, with the corrosion products forming at or above the liquid level. The conventional and as-received A1035 specimens exhibit significant corrosion products, such as shown for conventional steel in Figures 20 and 21, respectively. The pickled A1035 bars exhibited somewhat more limited corrosion products, as shown in Figures 22 and 23. The "grooves" along the length of the pickled specimens seem to provide a crevice at which corrosion initiates, with the corrosion products distributed along the length of the bar above the liquid level (Figures 22 and 23). This was not observed with the as-received bars, most likely due to the initial, corroded state of those specimens.

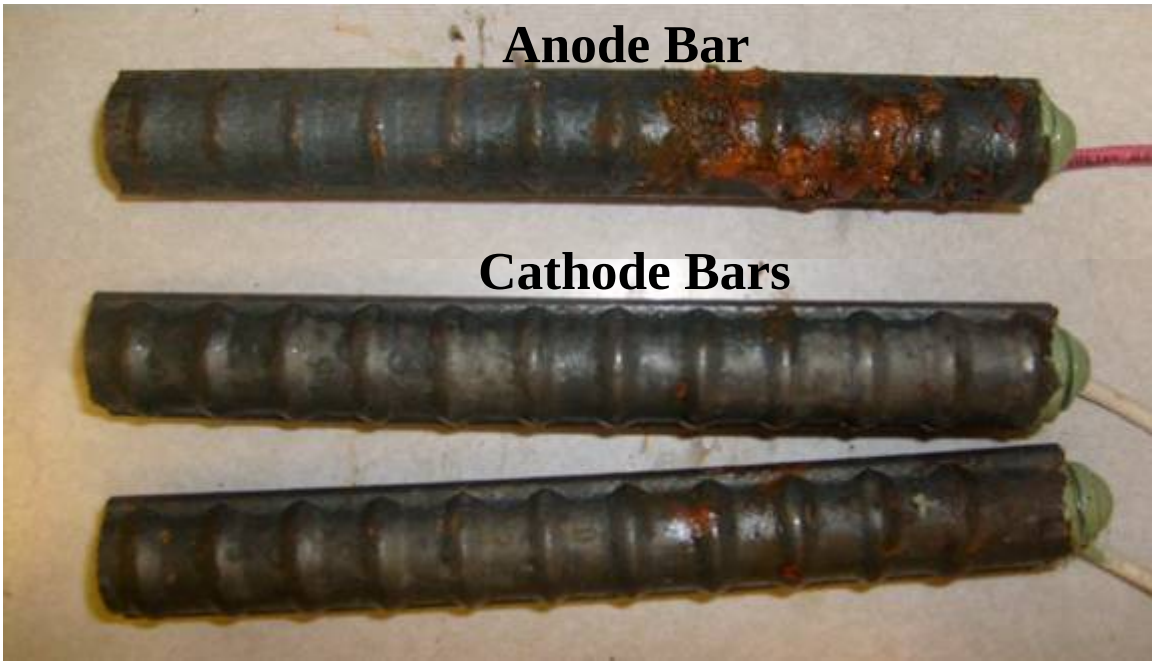

Figure 20: Conventional steel. Specimen 3, side A one week after removal from solution, after rinsing. Specimen exhibits significant corrosion above the liquid level.

Figure 21: A1035 steel. Specimen 3, side B one week after removal from solution, after rinsing. Specimen exhibits significant corrosion above the liquid level.

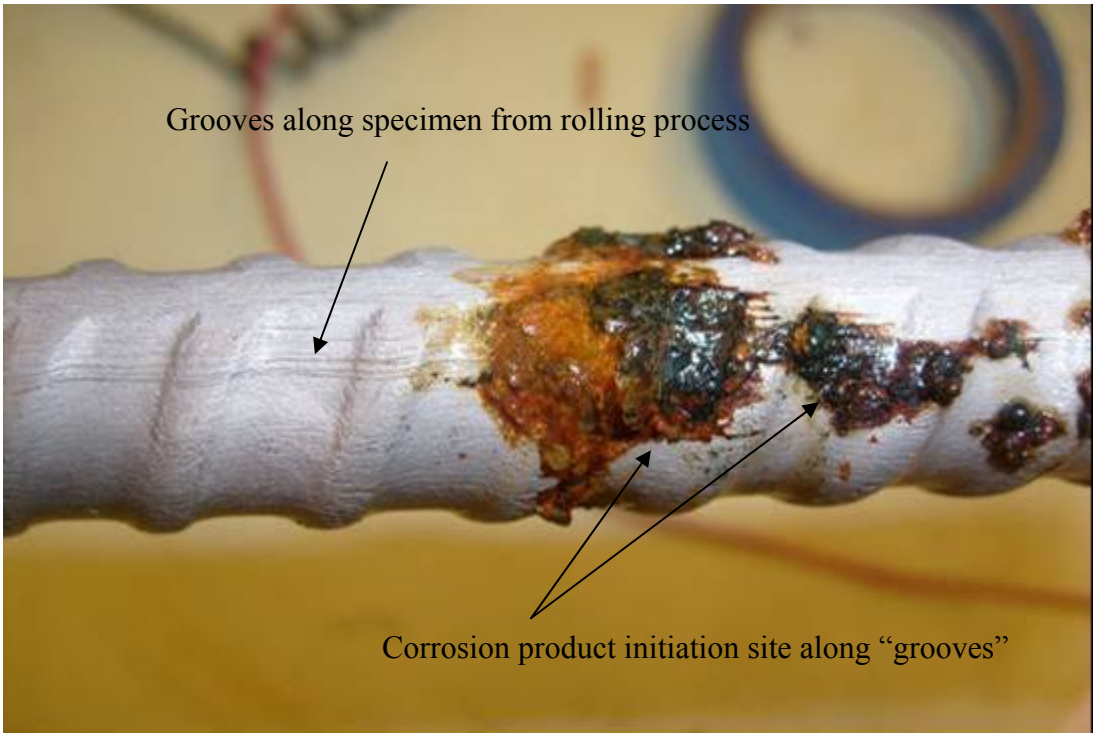

Figure 22: Pickled A1035 steel. Specimen 1 after removal from solution and rinsing.

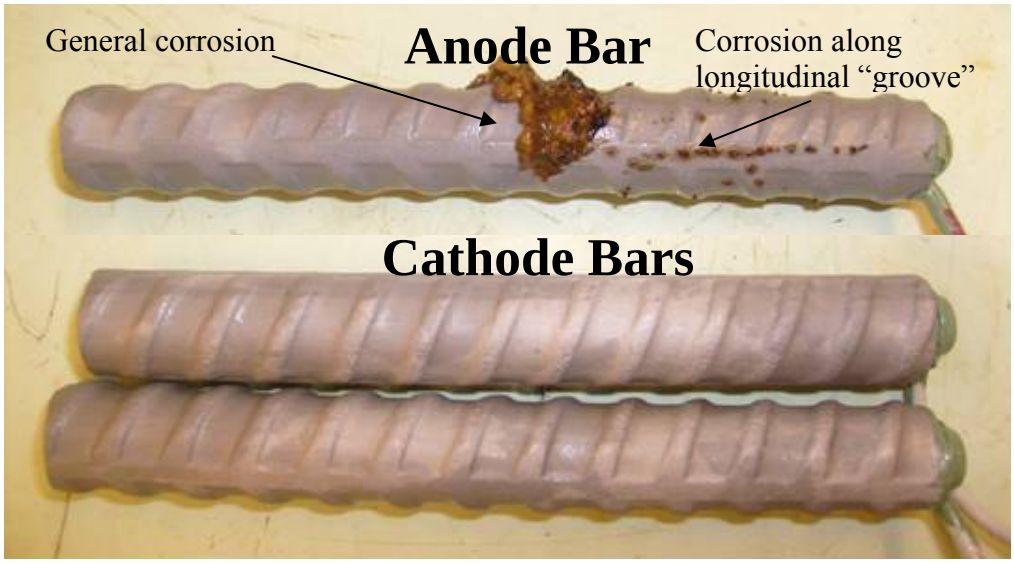

Figure 23: Pickled A1035 steel. Specimen 3, side A after removal from solution and rinsing.

Epoxy-Coated Reinforcing Steel

The individual corrosion rates of the six undamaged ECR specimens are shown in Figure 23, and the average corrosion rate is shown in Figure 24. Both individual and average corrosion rates are nearly zero. The "spikes" in the weekly readings shown in Figure 23 occur as the voltage readings range in and out of the 0.003-mV data filter described following Eq. (2).

The individual ECR specimens with the 0.04% damaged area exhibit corrosion rates in the range of –0.3 μm/yr to 0.3 μm/yr, with just a few exceptions, as shown in Figure 25, with the principal exceptions occurring on day 4 for specimens 1, 2, and 6, which exhibited spikes to 2.472 μm/yr, 4.288 μm/yr, and 7.782 μm/yr, respectively. These results, however, are likely due to faulty or corroded resistors and switches. Prior to testing, all switch boxes are cleaned and checked to ensure that they are in proper working order. After these faulty readings, however, the switch box in question was cleaned again, the terminals were cleaned or replaced, and selected switches and resistors were replaced. After the additional maintenance, no more errant readings were observed, and as a preventative measure, the resistances across the switches were checked for any suspect readings thereafter. Because of these observations, the three data points are not included in the average corrosion rate plot (Figure 26). These data points are included in Figure 25, but the y-axis is scaled to match that in the undamaged ECR plots; so these points are not shown. The average corrosion rate plot is very similar to the undamaged case and remains nearly zero throughout most of the test, although the range of the readings is higher than shown in Figure 24.

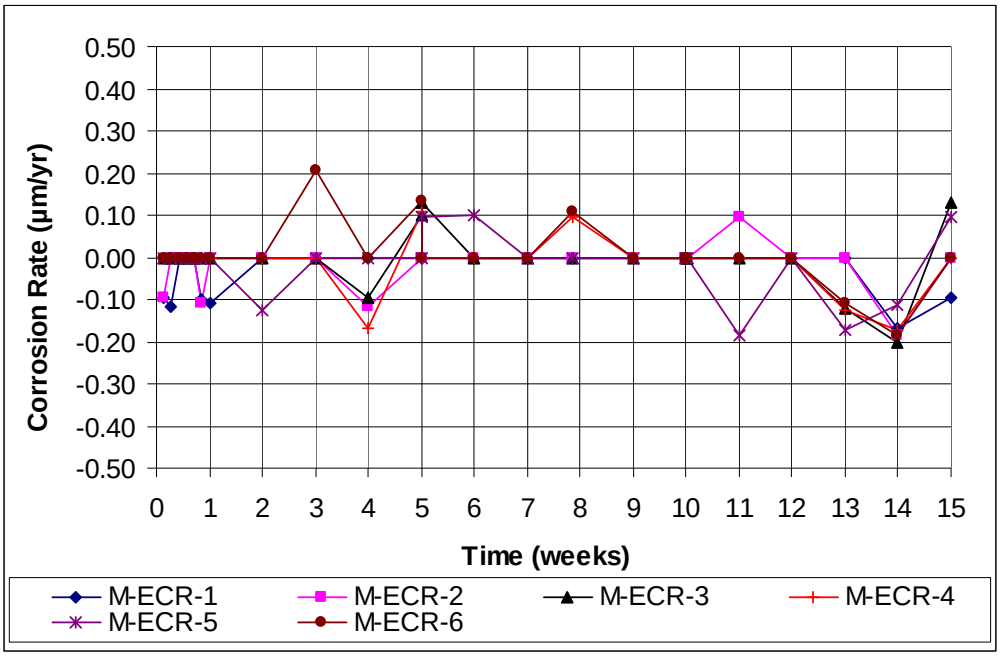

Figure 23: Individual corrosion rate of undamaged ECR, Specimens 1-6.

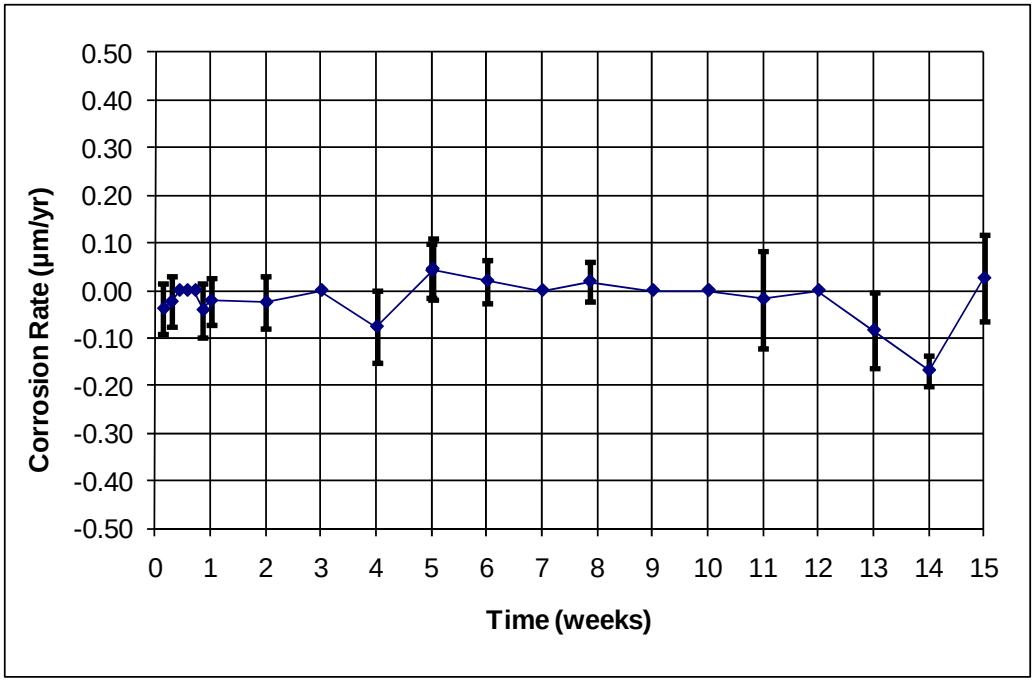

Figure 24: Average corrosion rate of undamaged ECR, Specimens 1-6.

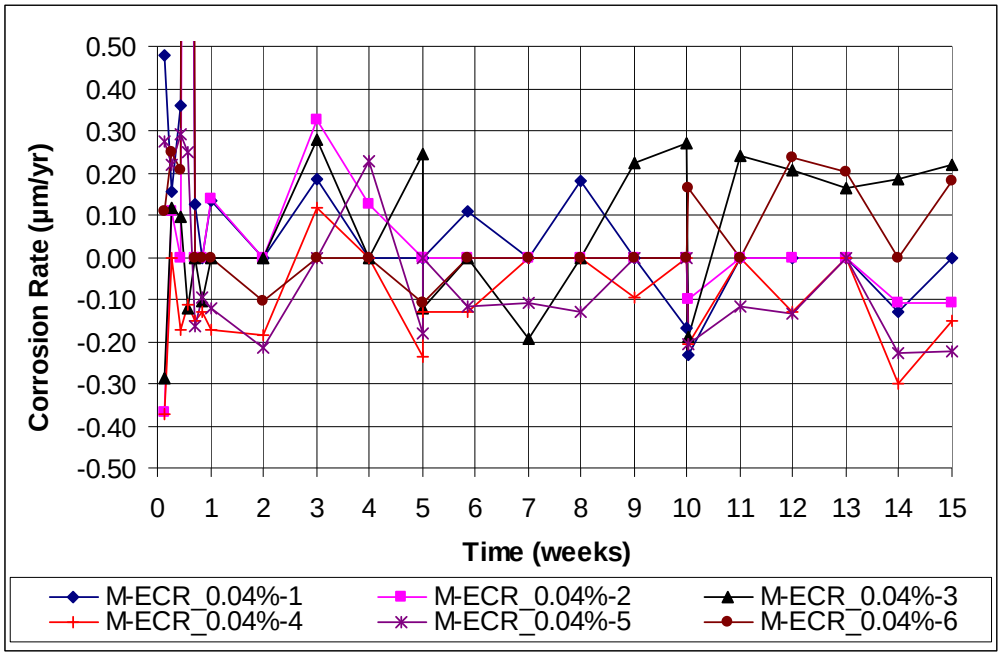

Figure 25: Individual corrosion rate of 0.04% damaged area ECR, Specimens 1-6.

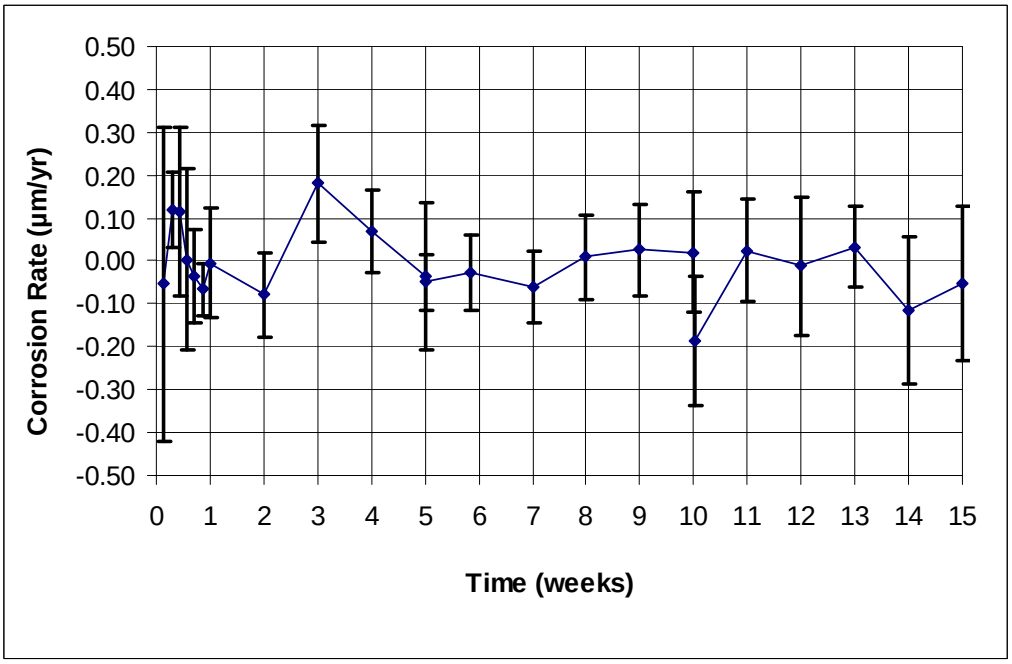

Figure 26: Average corrosion rate of 0.04% damaged area ECR, Specimens 1-6.

For the ECR with the 0.83% damaged area, individual corrosion rates (Figure 27) are higher than those for the undamaged or 0.04% damaged area ECR bars, with values ranging primarily from 0 to 4 µm/yr. The average corrosion rate ranges from 1 µm/yr to 1.5 µm/yr, as shown in Figure 28. The 0.83% damaged area ECR specimens used the same switch box as the 0.04% damaged specimens and had similar initial issues with readings. Specimen 2 exhibited a corrosion rate of 9.39 µm/yr on day 4 for the same reasons stated above, this value was determined to be an errant reading and is not included in the average corrosion rate plot.

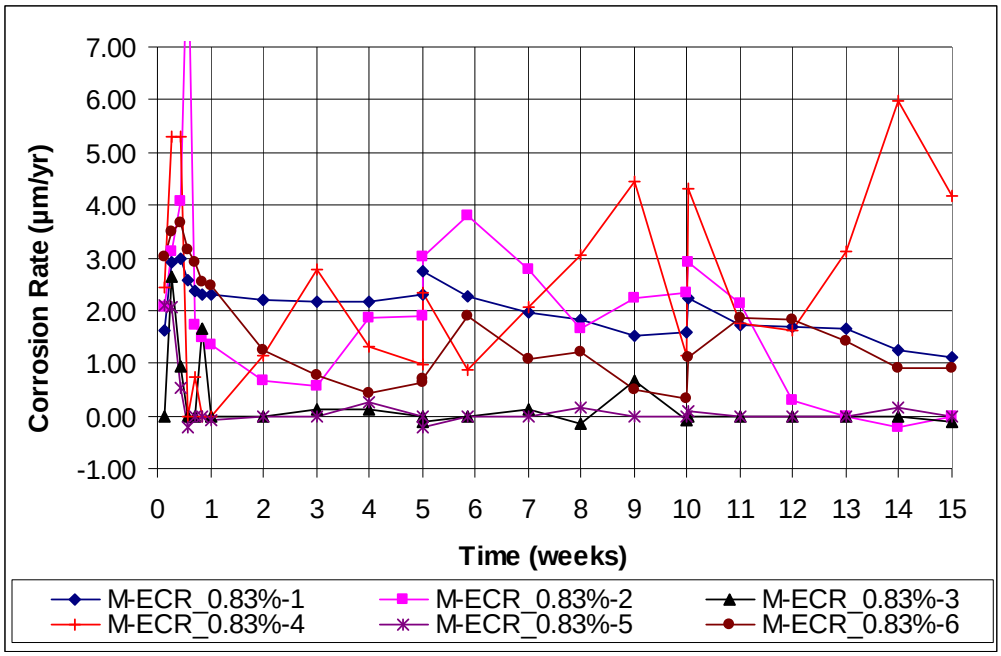

Figure 27: Individual corrosion rate of 0.83% damaged area ECR, Specimens 1-6 with a different y-axis scale.

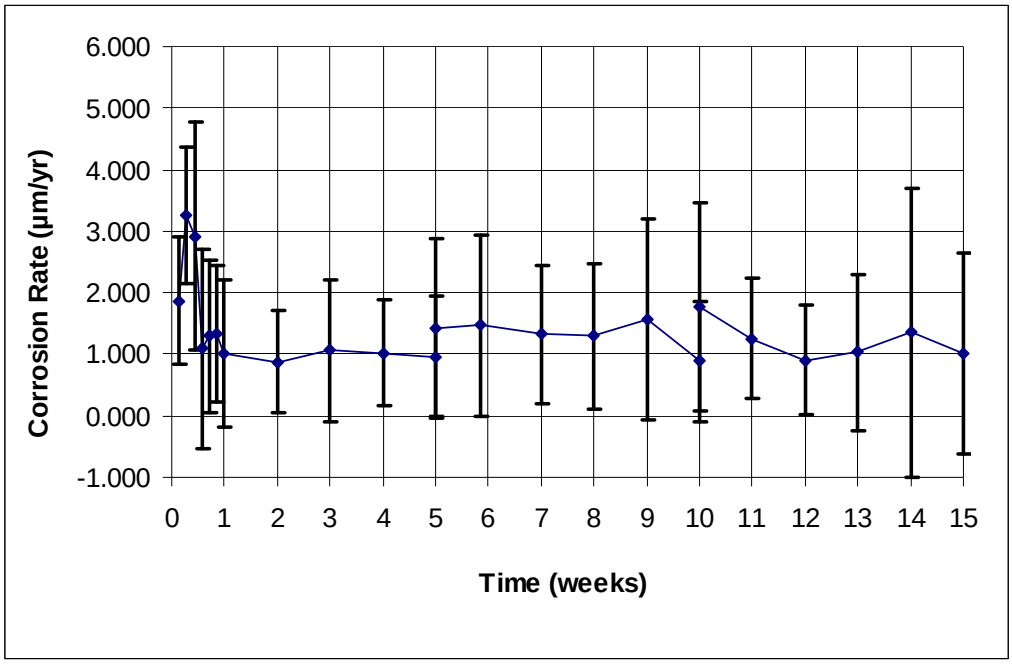

Figure 28: Average corrosion rate of 0.83% damaged area ECR, Specimens 1-6 with a different y-axis scale.

The individual corrosion potentials with respect to an SCE for the undamaged ECR specimens are shown in Figures 29 and 30 for the anode and cathode bars, respectively. The potentials exhibit large scatter, most likely because the undamaged epoxy coating blocks the ionic connection between the SCE and the specimen being tested. Anode potentials vary from –0.050 to –0.400 V, with the trend of becoming more negative as the tests progress. One exception is specimen 6, with an anode potential of –0.600 V for the majority of test. This is indicative of corrosion at the coating defect. After the test, specimen 6 was found to have an undetected holiday in the coating. For this reason, specimen 6 is not included in either the average corrosion rate plot or the average anode and cathode potential plots, although its corrosion rate remained low throughout most of the test, rising to 0.21 µm/yr for one reading (week 3). The cathodes remain relatively stable at –0.200 V for most of the test, with the exceptions of specimens 3 and 5, which exhibit potentials below –0.300 V from week 9 to 15

and 11 to 14, respectively. When examining specimens 3 and 5 at the end of the test, cracks were observed in the coating on the electrical connection, possibly contributing to the drop in potential. The average corrosion potentials for the undamaged ECR specimens are shown in Figure 31.

While similar to the undamaged ECR in corrosion rate, the 0.04% damaged area ECR specimens exhibit significantly more negative anode potentials than do the undamaged bars, with anode potentials near or below –0.600 V for five out of six of the specimens, as shown in Figure 32. Most of the specimens initiate between near –0.200 and –0.500 V, dropping to –0.600 V by the end of week 1 and remaining close to that potential for the balance of the test. Specimen 4 remains at approximately –0.200 V throughout the test and is the specimen with the lowest corrosion rate as well. The cathode potentials are shown in Figure 33 and are comparable to those for conventional steel. The average potentials are shown in Figure 34.

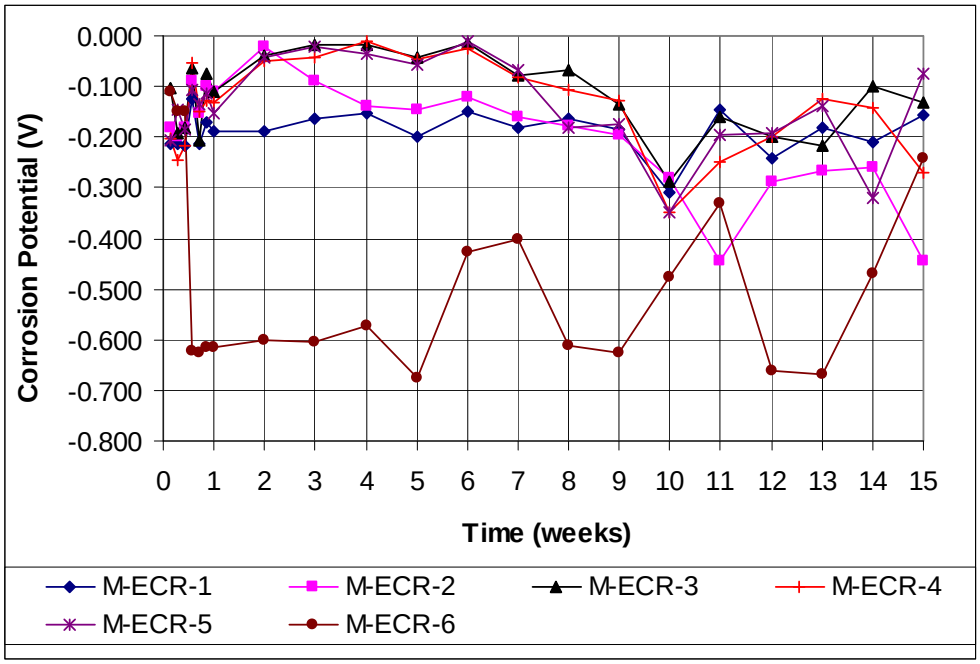

Figure 29: Individual corrosion potential with respect to SCE. Undamaged ECR in salt solution (anode), specimens 1-6.

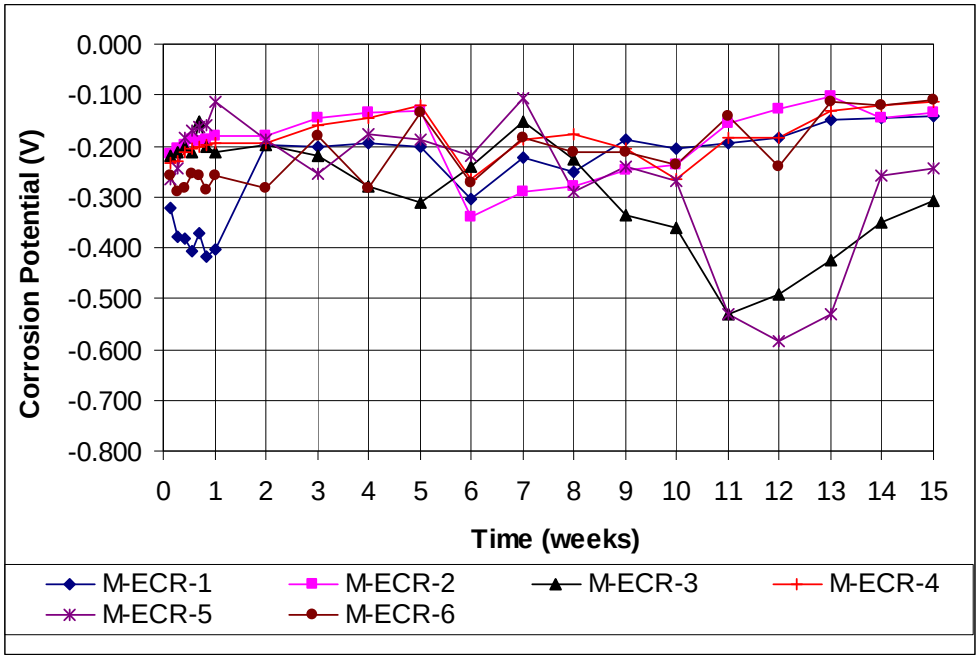

Figure 30: Individual corrosion potential with respect to SCE. Undamaged ECR in pore solution (cathode), specimens 1-6.

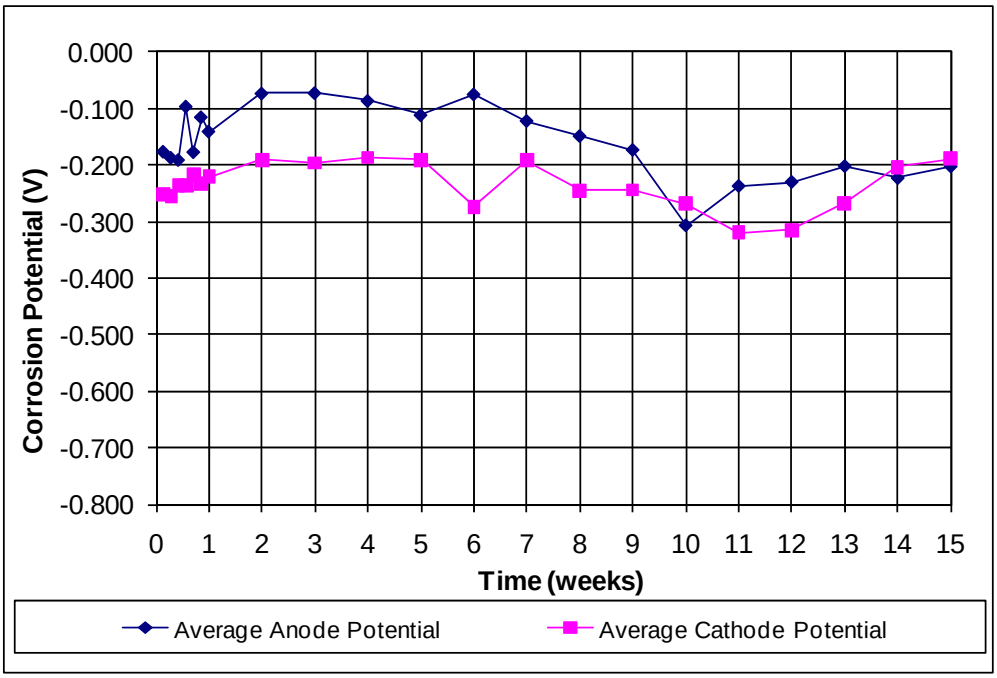

Figure 31: Average corrosion potential with respect to SCE. Undamaged ECR, specimens 1-6.

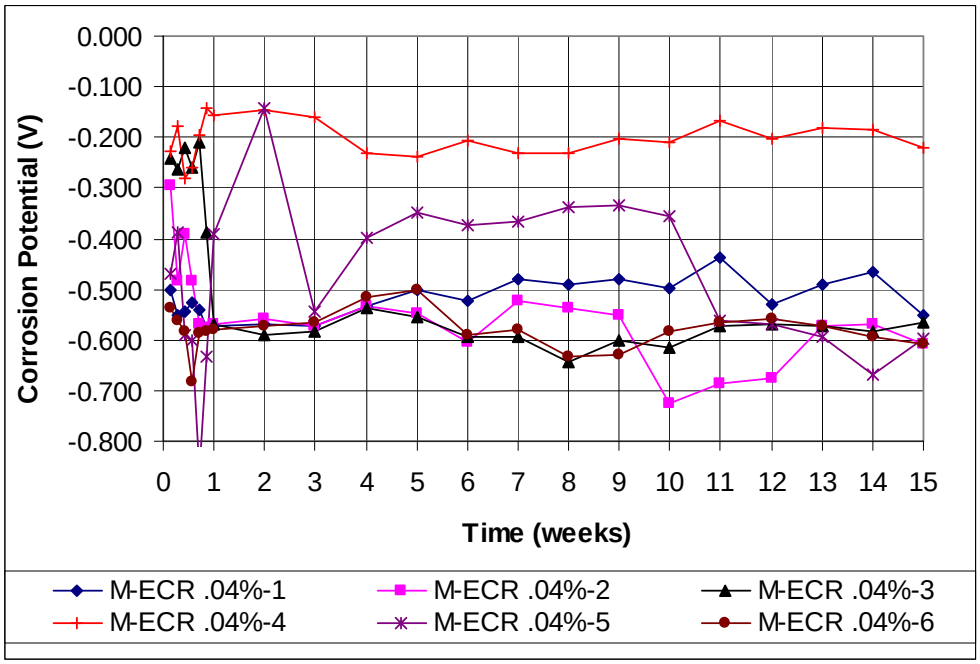

Figure 32: Individual corrosion potential with respect to SCE. 0.04% damaged area ECR in salt solution (anode), specimens 1-6.

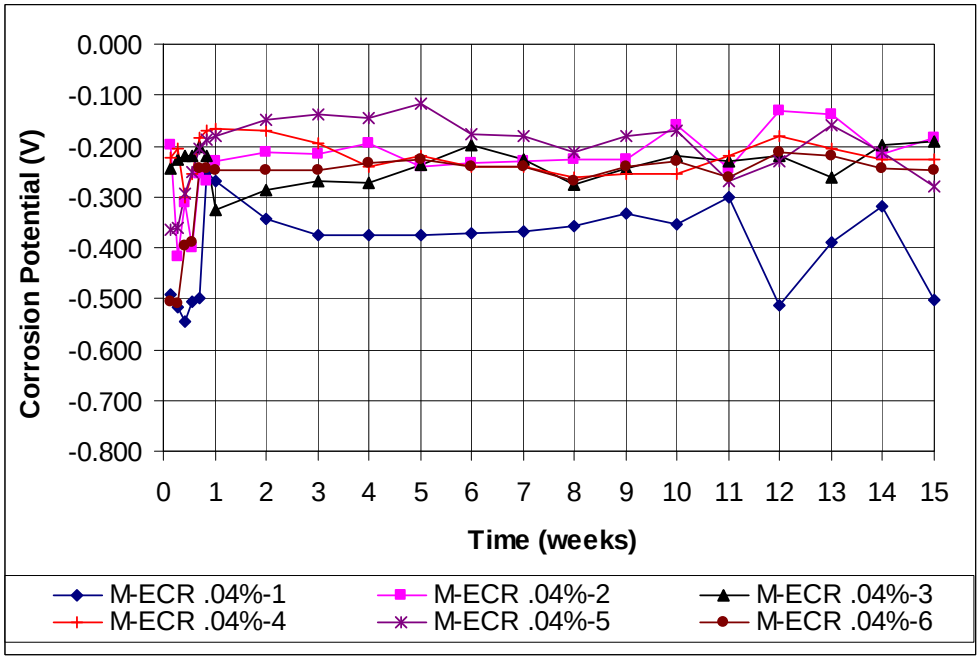

Figure 33: Individual corrosion potential with respect to SCE. 0.04% damaged area ECR in pore solution (cathode), specimens 1-6.

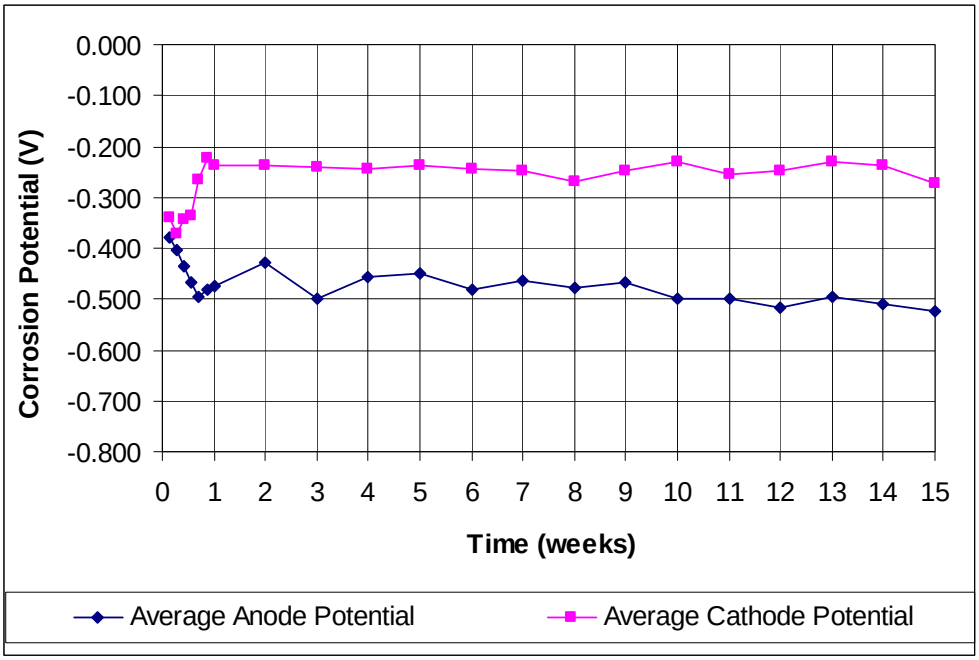

Figure 34: Average corrosion potential with respect to SCE. 0.04% damaged area ECR, specimens 1-6.

Corrosion potentials for the 0.83% damaged area ECR bars are similar to those of the 0.04% damaged area bars, with anode potentials (Figure 35) for most specimens close to –0.600 V, indicating corrosion at the damage location. The cathode potentials (Figure 36) are also similar with values of –0.250 to –0.300 V. The average potential values are shown in Figure 37.

Overall, the 0.04% damaged area ECR bars perform much like the undamaged ECR bars. Corrosion rates, however, exhibit greater scatter, and little corrosion is exhibited around the electrical connections. The corrosion rates for the 0.83% damaged area ECR bars are nearly ten times higher than for the 0.04% damaged area ECR bars; these bars, however, still provide over an order of magnitude improvement in corrosion resistance when compared with conventional steel reinforcement.

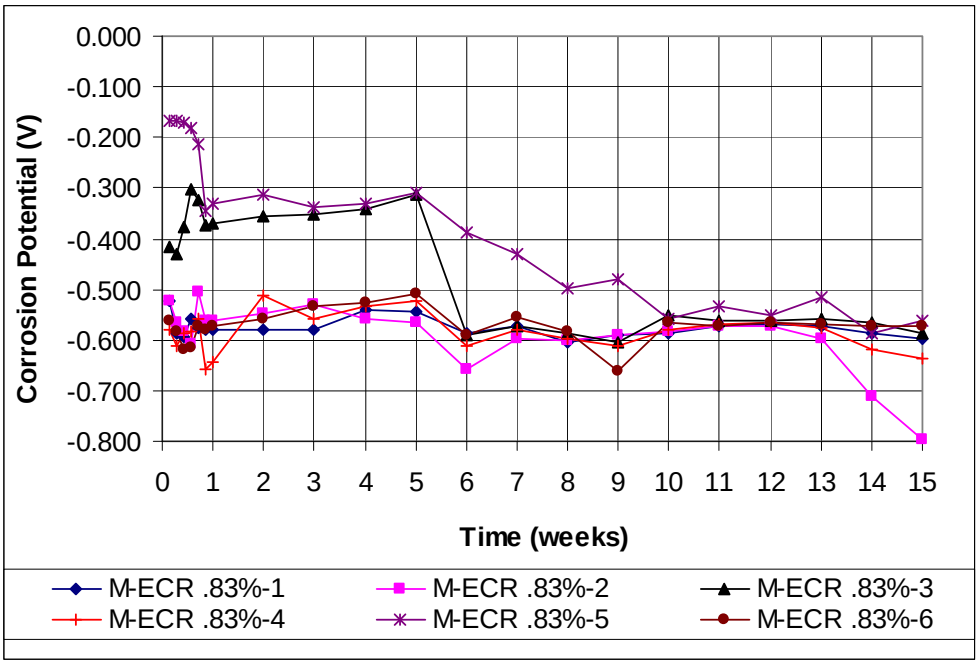

Figure 35: Individual corrosion potential with respect to SCE. 0.83% damaged area ECR in salt solution (anode), specimens 1-6.

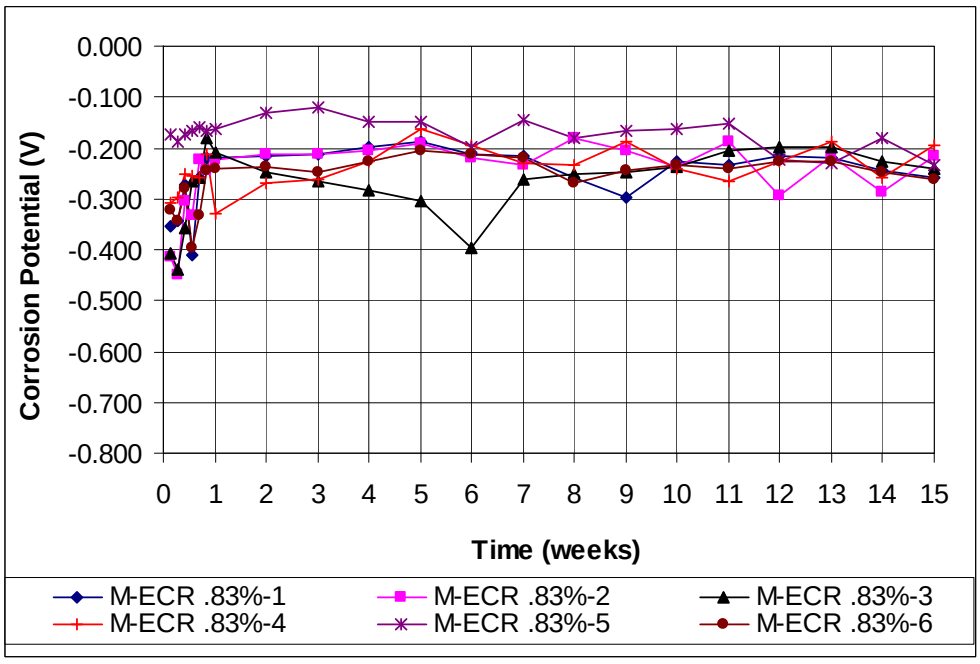

Figure 36: Individual corrosion potential with respect to SCE. 0.83% damaged area ECR in pore solution (cathode), specimens 1-6.

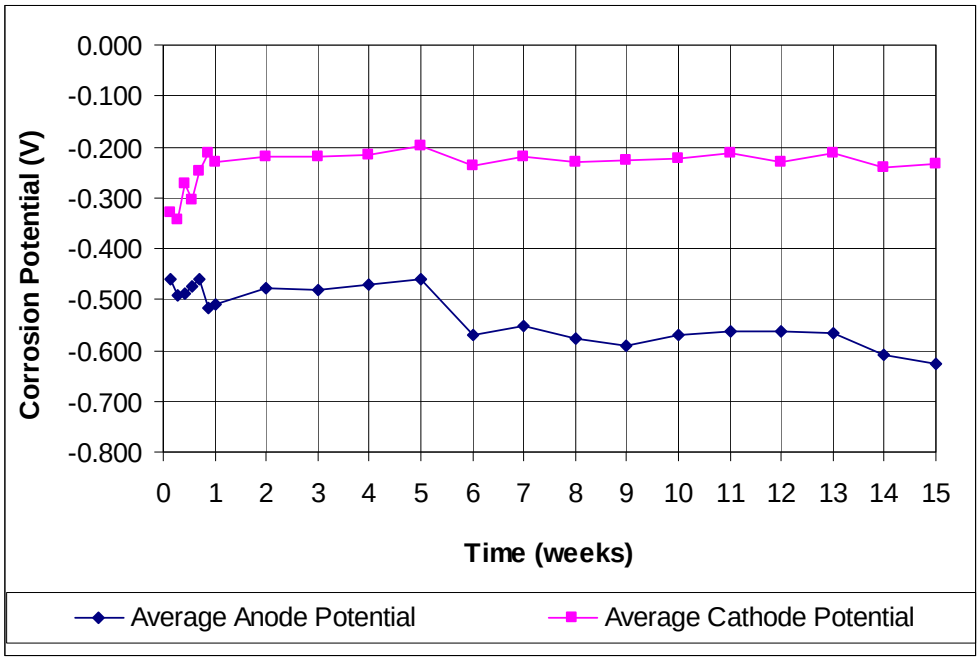

Figure 37: Average corrosion potential with respect to SCE. 0.83% damaged area ECR, specimens 1-6.

At the end of the test, the ECR specimens are inspected for corrosion and a disbondment test is performed on the anode bars. The results of the disbondment tests are covered in Appendix A. Figure 38 shows the deposition of corrosion products that is typical of that observed on the 0.83% damaged area ECR specimens at the conclusion of the test. Some damaged areas exhibited corrosion and some did not. In all cases, the epoxy remained intact. Corrosion was observed on some bars at the electrical connection with the copper wire, where the bar is coated with the two-part epoxy patch material. Examples are shown in Appendix A.

Figure 38: Corrosion typical of that seen on 0.83% damaged area ECR at conclusion of the test. Specimen 5, side A.

SUMMARY AND CONCLUSIONS

The corrosion performance of epoxy-coated steel meeting the requirements of ASTM A775 in the undamaged and two damaged conditions (0.04% and 0.83% damaged area) was tested using the rapid macrocell test in accordance with Annexes A1 and A2 of ASTM 955-10 and compared with that of conventional reinforcing steel meeting the requirements of ASTM A615 steel and low-carbon, chromium steel meeting the requirements of A1035, with the latter in both the as-received and pickled conditions.

The following conclusions are based on the test results presented in this report:

1. The macrocell corrosion rates for conventional A615 steel range from 10 to nearly 80 μm/yr, with an average of about 30 μm/yr.
2. The macrocell corrosion rates for A1035 steel in the as-received condition range from 10 to 40 μm/yr, with an average of about 20 μm/yr. For the pickled condition, the rates range from 0 to 25 μm/yr with an average of about 12 μm/yr.

3. Pickling provides initial protection to A1035 steel bars, and to some bars for the duration of the test, but once corrosion initiates, corrosion appears to be similar to that observed on non-pickled bars.
4. Epoxy-coated bars provide significantly better corrosion performance than conventional reinforcing steel.
5. The macrocell corrosion rates for bars with a damaged area equal to 0.04% of the area exposed to the solutions in the test are relatively low, and are, on average, similar to those observed for the undamaged epoxy-coated bars.
6. Both undamaged and 0.04% damaged area epoxy-coated specimens meet the requirements for stainless steels specified in Annexes A1 and A2 of ASTM 955-10, with an average corrosion rate not exceeding 0.25 μm/yr and the corrosion rate of no individual specimen exceeding 0.50 μm/yr.
7. The macrocell corrosion rates for bars with a damaged area equal to 0.83% of the area exposed to the solutions in the test average 1 to 1.5 μm/yr based on total bar area.

REFERENCES

ASTM A615, 2009, "Deformed and Plain Carbon-Steel Bars for Concrete Reinforcement (ASTM A615/A615M – 09b)," ASTM International, West Conshohocken, PA, 6 pp.

ASTM A775, 2007, "Epoxy-Coated Steel Reinforcing Bars (ASTM A955/A955M – 07b)," ASTM International, West Conshohocken, PA, 11 pp.

ASTM A955, 2010, "Standard Specification for Plain and Deformed Stainless-Steel Bars for Concrete Reinforcement (ASTM A955/A955M – 10)," ASTM International, West Conshohocken, PA, 11 pp.

ASTM A1035, 2009, "Standard Specification for Deformed and Plain, Low-carbon, Chromium, Steel Bars for Concrete Reinforcement (ASTM A1035/A1035M – 09)," ASTM International, West Conshohocken, PA, 5 pp.

ASTM C876, 2009, "Standard Test Method for Corrosion Potentials of Uncoated Reinforcing Steel in Concrete (ASTM C876 – 09)," ASTM International, West Conshohocken PA, 7 pp.

APPENDIX A

DISBONDMENT TESTS AND CORROSION AT ELECTRICAL CONNECTIONS

The disbondment test consists of slicing an "X" in the ECR coating using a pen-knife at the four damage sites, or where the damage site would be for the undamaged bars. Damage site 1 is located 1 in. from the bottom between two deformations on side A, and damage site 2 is located 1 in. above site 1 between two deformations on side A. Damage sites 3 and 4 are similar to sites 1 and 2, respectively, but on side B of the specimen. An attempt to peel back the epoxy coating is made until either the coating will no longer peel back or a longitudinal rib is reached in the circumferential direction and the second deformation above or below the damage site is reached along the specimen. The disbonded area (not including the original area where the epoxy is penetrated) is measured using 0.01 $in.^2$ grid paper, and the area is converted to square millimeters. Tables A1a, b, and c show the values of disbonded area for the undamaged, 0.04% damage area, and 0.83% damage area ECR bars, respectively.

Table A1a: Disbonded area (mm^2) for undamaged ECR specimens 1-6.

Specimen	1	2	3	4	5	6
Site 1	ND	ND	ND	ND	ND	ND
Site 2	ND	ND	ND	ND	ND	155
Site 3	ND	ND	ND	ND	ND	ND
Site 4	ND	ND	ND	ND	ND	ND

Note: 1.0 mm^2 = 0.00155 $in.^2$ ND = no disbondment

Table A1b: Disbonded area (mm^2)* for undamaged for 0.04% damaged area ECR specimens 1-6.

Specimen	1	2	3	4	5	6
Site 1	29	25	19	ND	25	90
Site 2	77	164	22	ND	77	93
Site 3	129	51	ND	ND	ND	25
Site 4	16	38	19	ND	106	ND

Note: 1.0 mm^2 = 0.00155 $in.^2$ *Values do not include area of original hole. ND = no disbondment

Table A1c: Disbonded area (mm^2)* for undamaged for 0.83% damaged area ECR specimens 1-6.

Specimen	1	2	3	4	5	6
Site 1	50	44	115	286	157	44
Site 2	366	605	105	208	102	186
Site 3	40	53	153	73	50	140
Site 4	70	457	47	47	50	263

Note: 1.0 mm^2 = 0.00155 $in.^2$ * Values do not include area of original hole.

As shown in the Table A1a, the undamaged ECR specimens exhibit disbondment at only one site (site 2 on specimen 6). The disbondment occurred at a previously undetected holiday in the specimen. This also accounts for the negative anode corrosion potential (~ –0.600 V) for that specimen. As mentioned in the report, this specimen is not included in the average corrosion rate and corrosion potential plots, but indicates that the presence of holidays can reduce corrosion performance. As shown in Tables A1b and c, the 0.04% damaged area ECR exhibits more limited disbondment than the 0.83% damaged area ECR, with respective average disbonded areas of 42 mm^2 and 155 mm^2. On both the 0.04% and 0.83% damaged area specimens, unintentional damage to the coating from the drilling process plays a role in the disbondment results. On occasion, the coating that was compressed by the grips during drilling of the anode bars provided additional sites for possible corrosion initiation. In particular, 0.04% damaged ECR specimen 1 (site 3), specimen 2 (site 2), and specimen 5 (site 5) exhibit increased disbondment due to this type of damage. Side 1 of specimen 1 is shown below in Figures A1 and A2. The relatively high disbondment shown in Figure A2 is in contrast to that which is more typical of 0.04% damaged ECR specimens, such as shown in Figure A3 for side 2 of specimen 2.

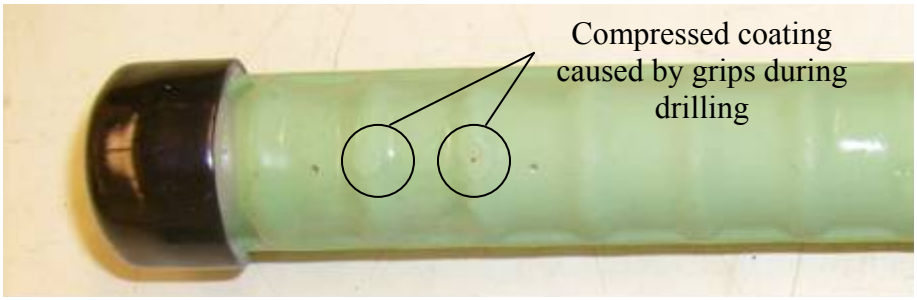

Figure A1: 0.04% ECR, specimen 2, side A. Before attempted disbondment.

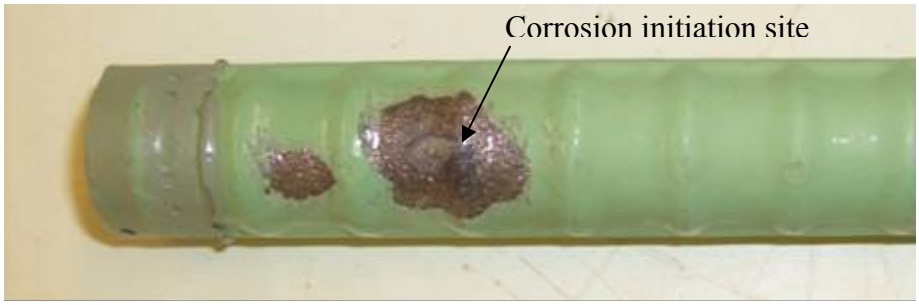

Figure A2: 0.04% ECR, specimen 2, side A. After disbondment.

Figure A3: 0.04% ECR, specimen 2, side B. After disbondment. Disbonded areas close to the average (42 mm^2) for 0.04% ECR specimens (see Table A1a).

As described above, the 0.83% damaged ECR bars exhibits more disbondment than either the undamaged or 0.04% damaged area bars (about 4 times greater than the latter). At times, disbondment extends to the other side of the bar. This is especially evident for 0.83% damage specimen 2, as shown in Figure A4. Compression of the epoxy coating also affects the disbondment in this case, although it is more difficult to pinpoint since generally more disbondment occurs at the intentional damage sites. The effect of compression of the coating on

disbondment, however, is clear on specimen 6 (site 2), shown in Figure A5, which exhibits significant disbondment away from the intentional damage sites. Other specimens apparently affected by compression of the coating include specimen 2 (sites 2 and 4), specimen 5 (site 1), and specimen 6 (site 4 in addition to site 2).

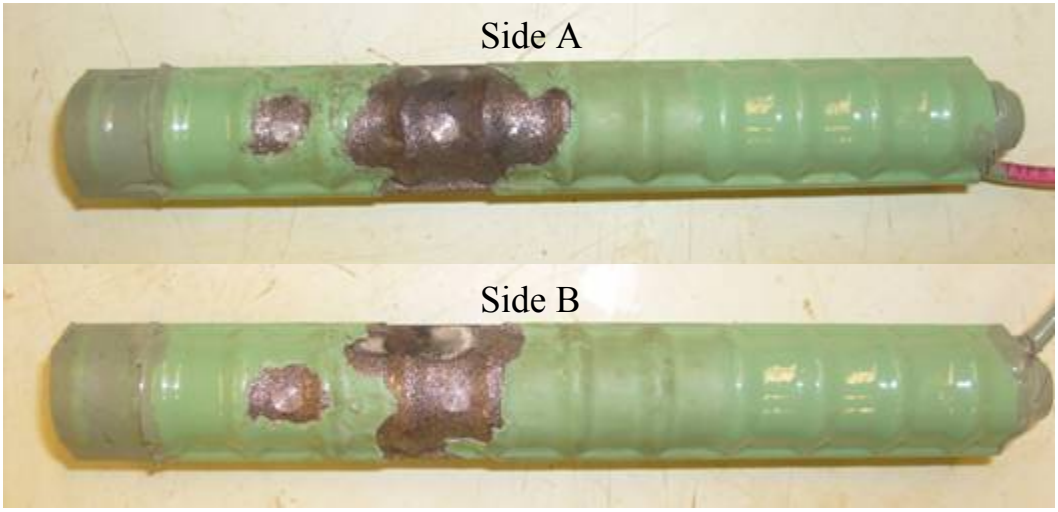

Figure A4: 0.83% ECR, specimen 2, after attempted disbondment.

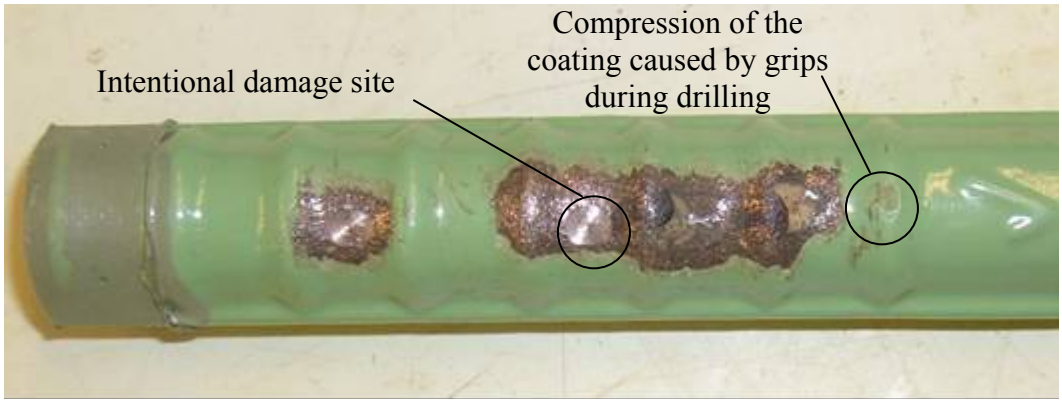

Figure A5: 0.83% ECR, specimen 6, after attempted disbondment.

For the undamaged ECR, no apparent corrosion occurs along the length of the specimens. Corrosion does occur, however, on some bars at the electrical connection with the copper wire, which is coated with the two-part epoxy patch material. The corrosion product is indicated by a slight visible surface rust on the steel and not corrosion of the copper wire, as shown in Figure

A6. Despite this local corrosion at the connection, the undamaged ECR performed very well. For example, undamaged ECR specimen 4 exhibits significant corrosion of the steel at the connection due to inadequate epoxy cover (Figure A7), but this corrosion has no appreciable effect on corrosion rate or potential, as shown in Figures 23 and 29.

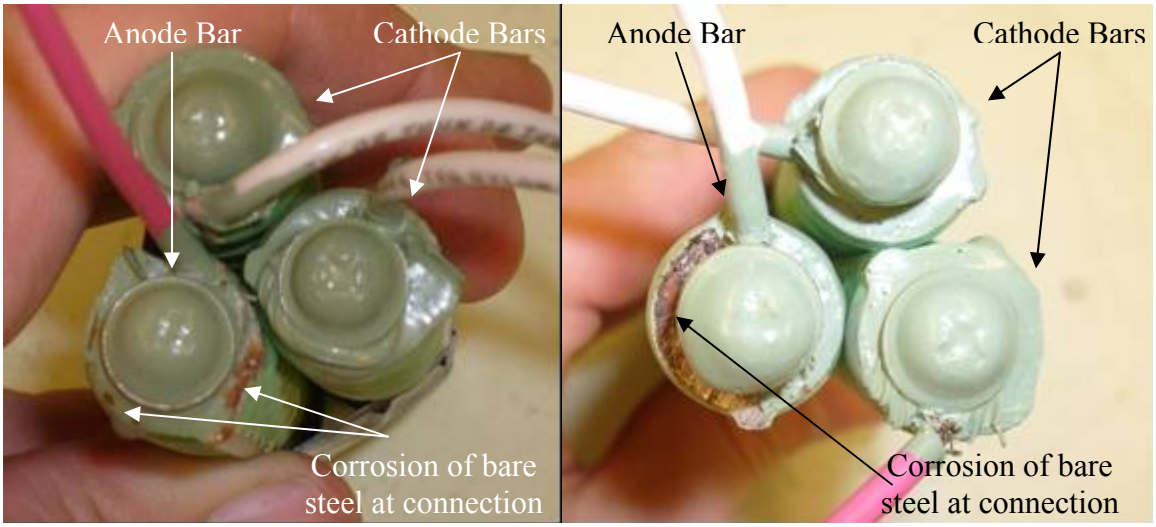

Figure A6: Undamaged ECR specimens. Left: Specimen 1, corrosion of bare steel occurs under the epoxy patch material. Right: Specimen 5, epoxy patch material is peeled back revealing corrosion of the bare steel.

Figure A7: Undamaged ECR, specimen 4 anode exhibits significant steel corrosion at the electrical connection.